Histol Histopathol (2025) 40: 1013-1039

Histology and Histopathology
From Cell Biology to Tissue Engineering

ORIGINAL ARTICLE Open Access

Identification of new tissue markers for the monitoring and standardization of penile cancer according to the degree of differentiation

Carlos Casanova-Martín[1,2*], Diego Liviu Boaru[1,2*], Oscar Fraile-Martinez[1,2], Cielo Garcia-Montero[1,2], Diego De Leon-Oliva[1,2], Patricia De Castro-Martinez[1,2], Maria José Gimeno-Longas[3], Julia Bujan[1,2], Natalio García-Honduvilla[1,2], Luis G. Guijarro[2,4], Raquel Gragera[1,2], Laura Lopez-Gonzalez[2,5], Miguel A. Saez[1,2,6], Connie Ferrara-Coppola[1,6], Víctor Baena-Romero[1,6], Raul Diaz-Pedrero[2,5,7], Melchor Alvarez-Mon[1,2,8], María Val Toledo-Lobo[2,9] and Miguel A. Ortega[1,2]

[1]Department of Medicine and Medical Specialities, Faculty of Medicine and Health Sciences, Network Biomedical Research Center for Liver and Digestive Diseases (CIBEREHD), University of Alcalá, Alcala de Henares, [2]Ramón y Cajal Institute of Sanitary Research (IRYCIS), [3]Department of Cell Biology, School of Medicine, Universidad Complutense de Madrid, Madrid, [4]Unit of Biochemistry and Molecular Biology, Department of System Biology (CIBEREHD), [5]Department of Surgery, Medical and Social Sciences, Faculty of Medicine and Health Sciences, University of Alcalá, [6]Pathological Anatomy Service, Central University Hospital of Defence-UAH Madrid, [7]Department of General and Digestive Surgery, General and Digestive Surgery, Príncipe de Asturias University Hospital, [8]Immune System Diseases-Rheumatology, Oncology Service an Internal Medicine (CIBEREHD), University Hospital Príncipe de Asturias and [9]Department of Biomedicine and Biotechnology, University of Alcalá, Alcalá de Henares, Spain
*Contributed equally

Summary. Penile cancer is an uncommon disease compared with other urological tumors and is more common in low- and middle-income countries. Risk factors include age, ethnicity, smoking, hygiene, and human papillomavirus infection. Although carcinoma of the penis can be cured in up to 80% of cases if detected early, late diagnosis drastically reduces survival rates, especially in metastatic cases. More than 95% of cases are squamous cell carcinomas, and the degree of cell differentiation is a key histopathological factor, distinguishing between poorly (P), moderately (M), and well-differentiated (W) carcinomas, with verrucous carcinoma (V) having the best prognosis due to its low metastatic capacity. This study analyses the differential expression of several biomarkers related to cell proliferation and cell cycle, inflammation, epigenetics, and autophagy (cell cycle (IRS-4, Ki-67, RB1, CDK4, cyclin D1, ERBB2, β-catenin, and MAGE-A), inflammation (COX2, NLRP3, and AIF-1), epigenetics (HAT-1) and autophagy (ULK-1 and ATG9A) in penile carcinoma according to the degree of differentiation. Immunohistochemical techniques were performed on 34 penile squamous cell carcinoma (PSCC) samples classified into subtype V (N=6), and groups P (N=9), M (N=9), and W (N=10). The findings suggest a differential expression of molecules according to the degree of cell differentiation, with a higher differential expression of molecules according to the degree of cell differentiation, suggesting that the proteins studied could have predictive value. The study highlights the complexity of PSCC and the need for future studies to explore translational applications and search for new biomarkers to improve clinical management and understanding of this disease.

Key words: Penile cancer, Biomarkers, Cell proliferation, Inflammation, Autophagy, Cell cycle, IRS-4, HAT-1, AIF-1

Corresponding Author: Miguel A Ortega, Department of Medicine and Medical Specialities, Faculty of Medicine and Health Sciences, Network Biomedical Research Center for Liver and Digestive Diseases (CIBEREHD), University of Alcalá, Alcala de Henares, Spain. e-mail: miguelangel.ortega@uah.es
www.hh.um.es. DOI: 10.14670/HH-18-846

Introduction

Carcinoma of the penis is a rare urological cancer in men compared with other more common tumors, such as prostate, (Sekhoacha et al., 2022), lung (Leiter et al.,

2023), or colorectal cancer (Shin et al., 2023). Epidemiological data show significant differences in the incidence of this type of cancer globally. Thus, countries such as Brazil or Uganda show higher incidence rates ranging from 2.9-6.8 and 3-4 per 100,000 men, respectively. In contrast, in the United States and Europe, the incidence rate is significantly lower, being 0.58, and 1.33 per 100,000 men, respectively (Morrison, 2014).

In Spain, the incidence rate of penile cancer is notably higher than in other European countries, amounting to 2.55 new cases per 100,000 men (Borque-Fernando et al., 2023). This disease generally affects older men, whose average age of diagnosis is approximately 70-80 years. Moreover, a higher incidence of this type of cancer is also observed in individuals of Hispanic descent compared with other ethnicities (Zhan et al., 2022). In addition to age and ethnicity, the main risk factors include smoking, poor hygiene, and phimosis (Morrison, 2014). Also, it is estimated that up to 20-50% of penile cancer cases are associated with infections caused by the human papillomavirus (HPV) (Iorga et al., 2020; Wei et al., 2023). The HPV serotype most associated with this type of cancer is HPV16, which accounts for up to 68.3% of infections caused by the virus, while HPV6 accounts for 8.1% and 6.9% of cases respectively (Olesen et al., 2019).

Diagnosis of penile cancer usually involves a visual inspection in which patients may notice changes in the glans or foreskin, even if they do not experience pain (Hakenberg et al., 2018). In addition, the clinician´s physical examination includes palpation of the penis and groin regions. The use of imaging techniques provides information on the extent and infiltration of the tumor, while diagnostic confirmation requires a biopsy (Hakenberg et al., 2015). Factors, such as tumor morphology, size and location, and the elimination of (micro)metastases in the inguinal lymph nodes are decisive factors for the stratification and clinical management of these patients (Protzel and Hakenberg, 2020). Early detection of penile cancer is crucial to avoid delays in treatment, however, late diagnosis is common, which negatively affects prognosis (Verhoeven et al., 2013). Difficulties in early diagnosis and accurate prognosis are due to the possibility that tumors may not be evident upon clinical examination, may be hidden by phimosis, the limitations of imaging techniques to detect micrometastases in clinically normal lymph nodes, and the lack of specific tumor markers (Hakenberg et al., 2015). Penile carcinoma can be cured in up to 80% of cases if detected early but the prognosis is dismal in metastatic cases, with five-year survival rates of less than 33% (Kellas-Ślęczka et al., 2019).

Pathologically, more than 95% of most malignant lesions of the penis are squamous cell carcinomas (Brouwer et al., 2023). The other tumors in this organ correspond to rare neoplasms, such as Kaposi´s sarcoma, cutaneous lymphomas, or different types of sarcomas (Thomas et al., 2021a). Within squamous cell carcinomas of the penis, several subtypes with different biological and clinical characteristics can be distinguished (Sanchez et al., 2015; Thomas et al., 2021a). According to their degree of histopathological differentiation, penile cancer can be divided into different subtypes, classified from worst to best prognosis: poorly differentiated tumors (P), moderately differentiated (M), and well-differentiated tumors (W) (Chaux et al., 2009; Teixeira Júnior et al., 2022). Conversely, verrucous carcinoma (V) is another entity of highly differentiated penile carcinoma, which is slow-growing and locally aggressive, but rarely metastasizes to nearby lymph nodes or distant locations, thus having a more favorable prognosis (Li et al., 2015). Further histopathological analysis of the different types of tumors may allow the identification of biomarkers useful in clinical practice and to guide specific therapies, promoting personalized and precision medicine (Bakhtiar, 2017; Duffy, 2013). The importance of certain histopathological and serum biomarkers in penile cancer is recognized, however, more research is needed to understand their implications in disease development and their potential clinical applications (Pekarek et al., 2022). In addition, few studies have investigated the differences and biomarker applications of different grades of penile cancer differentiation, suggesting that a comparative analysis of molecular characteristics may be beneficial to better understand the clinical and biological differences between these entities and to develop specific clinical applications.

Hanahan and Weinberg described the hallmarks of cancer, the set of characteristics and mechanisms associated with tumor development and progression (Hanahan and Weinberg, 2011). In its latest update (Hanahan, 2022), up to 14 hallmarks of cancer are recognized, including uncontrolled cell proliferation, cancer-associated inflammation, metabolic dysregulation, and non-mutational epigenetic reprogramming. A variety of molecules have been recognized to play a role in each of these mechanisms, which are also interrelated. For example, among the molecules involved in uncontrolled cell proliferation, this study has highlighted the role of molecules such as IRS-4 (insulin receptor substrate 4), Ki-67, RB1 (retinoblastoma), CDK4 (cyclin-dependent kinase 4), cyclin D1, ERBB2 (human epidermal growth factor receptor 2), β-catenin, and MAGE-A (melanoma antigen gene). Ki-67, RB1, CDK4, and cyclin D1 are biomarkers that tightly regulate cell cycle entry and progression and modulate cell proliferation processes (Hooper, 1994; Sun and Kaufman, 2018; Montalto and De Amicis, 2020; Goel et al., 2022; Ortega et al., 2022b;). IRS-4, ERBB2, β-catenin, and MAGE-A are involved in the regulation of several signaling pathways that promote cell proliferation and resistance to apoptosis (Weon and Potts, 2015; Zhang and Wang, 2020; Guijarro et al., 2023; Raghav and Moasser, 2023). In parallel, COX2 (cyclooxygenase-2), AIF-1 (allograft inflammatory

factor 1) and NLPR3 (NOD-like receptor pyrin domain 3) play a crucial role in promoting inflammation in the tumor microenvironment and participate in cancer progression and proliferation (Zhao et al., 2013; Hashemi Goradel et al., 2019; Liu et al., 2019). Furthermore, HAT-1 (histone acetyltransferase 1) is an enzyme potentially involved in the epigenetic dysregulation of different types of tumors while ULK-1 (Unc-51-1-like autophagy activating kinase) and ATG9A (autophagy-related protein 9A) are involved in the reprogramming of tumor metabolism (specifically regulating autophagy). These are processes that facilitate cell survival and adaptation under adverse conditions involved in cancer development and progression (Claude-Taupin et al., 2021; Poziello et al., 2021; Shen et al., 2022).

Some studies have suggested the potential involvement of some of these molecules is altered in penile squamous cell carcinomas (PSCCs), such as Ki-67 (Berdjis et al., 2005), RB1 (da Silva et al., 2022), cyclin D1 (Ioachim, 2008), CDK4 (McDaniel et al., 2015), ERBB2 (Tan et al., 2023), MAGE (Hudolin et al., 2006), and COX2 (De Paula et al., 2012), while the possible role of other molecules such as IRS-4, AIF-1, NLRP3, HAT-1, ULK-1, and ATG9 has, to the best of our knowledge, not yet been studied. In this sense, our starting hypothesis is that there is a differential expression of previously described markers in penile carcinoma according to their degree of differentiation, as well as of molecules not yet explored in this type of tumor but whose relevance in cancer is widely proven by previous works. Similarly, we also hypothesize that each tumor subtype included in this study has different molecular correlations that may help to understand the differences in the biological behavior of each. Finally, we propose that the analysis of the expression levels of each molecule can be specifically related to each cancer subtype and that they could serve as diagnostic biomarkers.

The present study aims to analyze the protein expression profiles of molecules in the different subtypes of penile cancer according to their degree of differentiation using immunohistochemical techniques. A total of 34 samples of PSCC will be analyzed, six corresponding to subtype V, nine to groups P and M, and 10 from group W.

Materials and methods

Study design and participants

Our research adopted an observational and analytical approach with a retrospective cohort design. Histological specimens of PSCC were collected from 34 patients undergoing surgery. Paraffin blocks were prepared for further study, and comprehensive clinical information on the patient was recorded. The diagnosis and clinical management of the patients were performed following the guidelines of the European Association of Urology (EUA) and the Society of American Oncology (SEOC) (Brouwer et al. 2023). In the present work, tumors were stratified based on their degree of differentiation, following the model proposed by the 8th edition of the UICC/AJCC TNM (Kranz et al., 2024). According to this system, a distinction is made between poorly (P), moderately (M), and well-differentiated (W) tumors. In parallel, paraffin-embedded sections were also obtained from patients with verrucous penile carcinoma (V). Table 1 details the number of patients included, mean age, and TNM classification for each group.

The study rigorously adhered to fundamental ethical principles, including autonomy, beneficence, non-maleficence, and distributive justice. Furthermore, it was conducted following the Good Clinical Practice guidelines and ethical standards outlined in the latest Declaration of Helsinki (2013) and the Oviedo Convention (1997). All data and information collected were handled in compliance with current data protection legislation, including Organic Law 3/2018 of 5 December on Personal Data Protection and Guarantee of Digital Rights, as well as Regulation (EU) 2016/679 (Table 1).

Immunohistochemical techniques

The antibody recovery process was carried out according to the specifications described in the protocol (Table 2). The detection of antigen-antibody reactions used the avidin-biotin complex (ABC) method, using avidin-peroxidase according to established protocols (Ortega et al., 2021). After incubation with primary antibody for 1 hour and 30 minutes, the samples were subjected to overnight incubation with 3% BSA blocker (catalog #37525; Thermo Fisher Scientific, Inc., Waltham, MA, USA) and phosphate buffer saline (PBS) at 4°C. Subsequently, samples were incubated with biotin-conjugated secondary antibody diluted in PBS for 90 min at room temperature (RT). Specifically, rabbit IgG, diluted 1:300 (RG-96; Sigma-Aldrich, St. Louis, MI, USA), goat IgG, diluted 1:100 (GT-34/B3148; Sigma-Aldrich), and mouse IgG, diluted 1:300

Table 1. Summary of the characteristics and data of patients included in this study.

Stadium	No. of patients	Average age ± SD	TNM	Ulcer
V	6	80.500±3.082	pT1a	No
W	10	71.500±9.823	pT2	Yes
M	9	78.222±11.681	pT2	Yes
P	9	74.889±10.080	pT2	Yes

Stage (V) refers to verrucous carcinoma, (W) well-differentiated carcinoma, (M) moderately differentiated, and (P) poorly differentiated. The mean ages of each group are shown with the corresponding standard deviation (SD). In addition, the TNM classification (tumor, lymph node, and metastasis) is shown, as well as the presence or absence of ulcers in each group.

(F2012/045K6072; Sigma-Aldrich) were used.

Thereafter, samples were subjected to ExtrAvidin® peroxidase conjugate (Sigma-Aldrich; Merck KGaA, Darmstadt, Germany) for 60 min at RT (diluted 1:200 with PBS). Protein expression levels were assessed using a diaminobenzidine (DAB) Chromogenic Substrate Kit (cat. no. SK-4100; Maravai LifeSciences, San Diego, CA, USA), freshly prepared before use. The peroxidase chromogenic substrate was applied for 15 min at RT, allowing the development of brown staining indicative of protein expression. For each protein, negative control sections were included, with incubation with the primary antibody replaced by blocking solution and PBS. Carazzi's hematoxylin staining was performed for 15 minutes at RT to provide contrast in all tissues (Table 2).

Histopathological analysis

Tissue sections were examined using a Zeiss Axiophot light microscope (Carl Zeiss, Oberkochen, Germany) equipped with an AxioCam HRc digital camera (Carl Zeiss, Oberkochen, Germany). Given the importance of the proteins under investigation, histological evaluations were performed according to the intensity of immunohistochemical staining using a scoring system.

The study of protein expression in different penile cancer types was evaluated using the immunoreactive score (IRS), as specified in previous protocols (Ortega et al., 2022a). Two independent pathologists evaluated the samples, and any discrepancies were resolved by a third pathologist. Each group of subjects was represented by seven microscopy fields randomly selected from five sections. Subjects were classified as positive if the mean proportion of labeled specimens exceeded or equaled 5% of the total sample. This determination was made by calculating the overall percentage of labeled tissue in each microscopy field to derive an average for the entire study sample (Fraile-Martinez et al., 2023).

Statistical analysis

For the analysis of the protein expression of the biomarkers in the different patients, a normality check was performed (Kolmogorov-Smirnoff, all $p<0.001$). Since we observed that they do not have a normal distribution, it was necessary to describe the results with medians and interquartile ranges by performing nonparametric tests, in this case, the Mann-Whitney U test. Next, to analyze the differential expression of the biomarkers studied among the different types of PSCC included, the Bonferroni multiple comparison test of means will be applied.

To perform a correlation analysis, the R statistical software was used, applying the corrplot operations package. The correlation matrix was prepared with Pearson's coefficients, whose significance levels were calculated with the corresponding cor.test. The software used was Rstudio version 2023.12.1 built 402. To estimate the odds ratio, we first performed a principal component analysis (PCA) with the scaled values from the previous correlation analysis, and then a multinomial logistic regression (MLR), also using RStudio. The main functions run were prcomp and multinom (nnet package), and lrtest (lmtest package), respectively. These approaches were designed to obtain the logarithms of the odds ratios of the transition from each group of patients to the other groups based on the IRS scores of the 14 protein markers evaluated. With the first step of PCA, we sought to reduce the dimensionality of the data set of 14 protein variables to two principal components (PCs) while maintaining the overall variation in protein expression profiles. We considered the limitations of the linear PCA assumption between variables and the lack of nonlinear capture of the relationships between them. In the second step, we ran the RLM from the PCA data. We interpreted the coefficients obtained from the RLM model as odds ratios (already given on a real scale without the need for exponentiation) understood as the

Table 2. Primary and secondary antibodies and their dilutions.

Antigen	Dilution	Supplier	Protocol specifications
IRS-4	1:500	Thermo Fisher Scientific – PA5-117329	Preincubation with Tris-EDTA Buffer pH 9 and incubation with 0.1% TTX (Triton x100 in TBS) for 5 minutes
Ki-67	1:1000	Vitro, MAD-000310QD-3/V	-
RB1	1:750	Vitro, MAD-000900QD-3/V	-
CDK4	1:250	Vitro, MAD-000597QD-3/V	-
Cyclin D1	1:500	Vitro, MAD-000630QD-3/V	-
ERBB2	1:500	Vitro, MAD-000308QD-3/V	-
ꭤ-catenin	1:250	Vitro, MAD-000699QD-3/V	-
MAGE-A	1:50	Santa cruz (sc-20034)	-
COX2	1:1000	Vitro, MAD-000335QD-3/V	-
NLPR3	1:500	Abcam (ab263899)	-
AIF-1	1:500	Abcam (ab5076)	EDTA pH 9 before incubation with blocking solution
ULK-1	1:500	Abcam (ab203207)	Sodium chloride 10 mM. pH 6, before incubation with the blocking solution
ATG9A	1:50	Abcam (ab108338)	100% Triton 0.1% in PBS for 10 minutes before incubation with the blocking solution
HAT-1	1:1000	Abcam (ab193097)	100% Triton 0.1% in PBS for 10 minutes before incubation with the blocking solution
IgG (Rabbit)	1:1000	Sigma-Aldrich (RG-96/B5283)	-
IgG (Mouse)	1:300	Sigma-Aldrich (F2012/045K6072)	-

relative transition probabilities between groups.

Results

Penile squamous cell carcinomas with a lower degree of tissue differentiation show a significant increase in proliferation and cell cycle markers

First, our results show an increase in the expression of the proliferation biomarker IRS-4; as the disease stage worsens, this marker increases its expression, as indicated by the IRS score (V=0.917±0.376; W= 1.650±0.412; M=2.056±0.300; and P=2.889±0.220 (Fig. 1A). Also, in the histological sections of the four stages, it can be seen that the concentration of IRS-4 expression increases and is found in greater proportion in the P group (Fig. 1B-E).

Next, we found that the expression of the proliferation marker Ki-67 intensifies as the disease worsened (Fig. 2A) (V=0.583±0.492; W=1.050±0.284; M=1.444±0.391; and P=2.111±0.333). In addition, in histological sections of the four stages, it can be seen that the concentration of Ki-67 expression increases and is found in greater proportion in the P group (Fig. 2B-E).

The next cell cycle biomarker studied was RB1, whose expression increases as the disease worsens (Fig. 3A) (V=0.417±0.376; W=1.100±0.211; M=1.222±0.363; and P=1.667±0.354). In addition, in histological sections of the four stages, it can be seen that the concentration of RB1 expression increases and is found in greater proportion in the P group (Fig. 3B-E).

We also observed that the expression of biomarker CDK4, a cell cycle marker, increases as the cancer stage becomes more undifferentiated (V=0.667±0.408; W=1.100±0.316; M=1.722±0.363; and P=2.222±0.507) (Fig. 4A). In addition, in histological sections of the four stages, it can be seen that the concentration of CDK4 expression increases and is found in greater proportion in the P group (Fig. 4B-E).

Another biomarker whose expression is studied in the development of penile cancer, and which belongs to the cell cycle group, is cyclin D1. Its expression increases as the disease worsens (Fig. 5A) (V= 0.833±0.258; W=1.300±0.483; M=1.722±0.363; and P=2.111±0.417). In addition, in histological sections of the four stages, it can be seen that the concentration of cyclin D1 expression increases and is found in greater proportion in the P group (Fig. 5B-E).

After that, the cell proliferation biomarker ERBB2 was studied; its expression increased as tumor development progressed (Fig. 6A) (V=0.917±0.376; W=1.650±0.474; M=1.833±0.433; and P=2.278±0.264). In addition, in histological sections of the four stages, it can be seen that the concentration of ERBB2 expression increases and is found in greater proportion in the P group (Fig. 6B-E).

We also studied the expression of the cell proliferation biomarker, β-catenin 1; the concentration of this biomarker increases as the stage of the disease differentiates (Fig. 7A) (V=0.750±0.274; W=1.200± 0.422; M=1.611±0.417; and P=2.167±0.250). In addition, in histological sections of the four stages, it can be seen that the concentration of β-catenin 1 expression increases and is found in greater proportion in the P group (Fig. 7B-E).

Finally, the expression of biomarker MAGE-A, related to cell proliferation, was observed. This marker appears to increase as tumor progression worsens (Fig. 8A) (V=1,167±0,408; W=1.950±0.284; M=2.222±0.507; and P=2.889±0.333). In addition, the histological sections of the four stages show that the concentration of MAGE-A expression increases and is found in greater proportion in the P stage (Fig. 8B-E).

The data were corroborated with the Bonferroni test, as shown in Table 3.

The expression levels of inflammatory proteins COX2, AIF-1, and NLRP3 inversely correlate with the degree of tumor differentiation of penile squamous cell carcinoma

First, our results show an increase in the expression of the proliferation biomarker COX2, as the disease stage worsens, this marker increases its expression, as indicated by the IRS score (V=0.583±0.492; W= 1.250±0.486; M=1.833±0.433; and P=2.111±0.417) (Fig. 9A). Also, in histological sections of the four stages, it can be seen that the concentration of COX2 expression increases and is found in higher proportion in the P group (Fig. 9B-E).

Next, we found that the expression of the proliferation marker AIF-1 intensifies as the disease worsened (Fig. 10A) (V=0.750±0.274; W=1.350±0.337; M=2.056±0.300; and P=2.389±0.546). In addition, histological sections of the four stages show that the concentration of AIF-1 expression increases and is found in greater proportion in the P group (Fig. 10B-E).

Finally, the expression of biomarker NLRP3, related to cell proliferation, was observed. This marker appears to increase as tumor progression worsens (Fig. 11A) (V=0.917±0.492; W=1.350±0.337; M=2.167±0.354; and P=2.778±0.441). In addition, in histological sections of the four stages, it can be seen that the concentration of NLRP3 expression increases and is found in greater proportion in the P group (Fig. 11B-E).

The data were corroborated with the Bonferroni test, as shown in Table 3.

Protein expression of the epigenetic protein HAT-1 and autophagy mediators ULK-1 and ATG9A inversely correlates with the degree of tumor differentiation of penile squamous cell carcinoma

First, our results show an increase in the expression of the proliferation biomarker HAT-1; as the disease stage worsens, this marker increases its expression, as indicated by the IRS score (V=0.667±0.606; W= 1.250±0.354; M=2.222±0.264; and P=2.944±0.167) (Fig. 12A). Also, in histological sections of the four

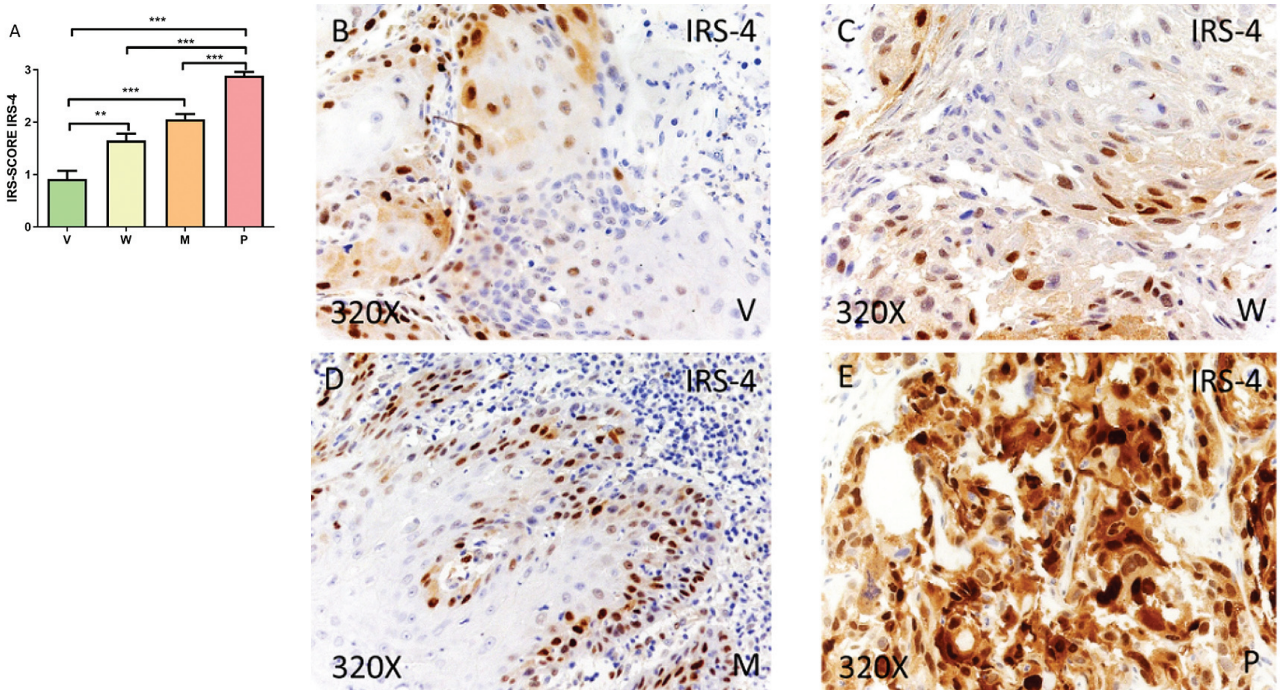

Fig. 1. A. Histological specimens were categorized as verrucous (V=0.917±0.376), well-differentiated (W=1.650±0.412), moderately differentiated (M=2.056±0.300), and poorly differentiated (P=2.889±0.220) expression levels using the IRS-Score method. Photomicrography showing the expression level of IRS-4 in verrucous penile carcinoma (V) **(B)**, in well-differentiated penile carcinoma (W) **(C)**, and in moderately differentiated penile carcinoma (M) **(D)**. **E.** Elevated expression levels of IRS-4 in poorly differentiated penile carcinoma (P). **p*<0.05, ***p*<0.01,****p*<0.001. x 320.

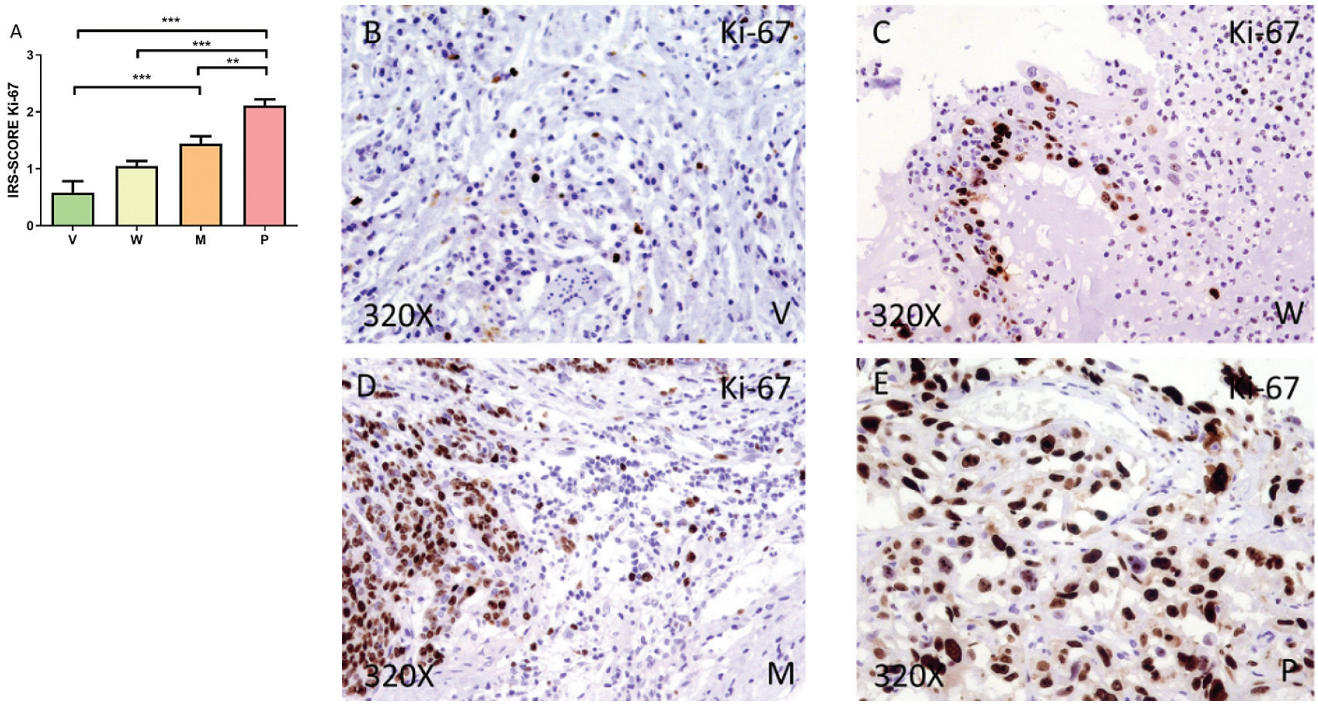

Fig. 2. A. Histological specimens were categorized into verrucous (V=0.583±0.492), well-differentiated (W=1.050±0.284), moderately differentiated (M=1.444±0.391), and poorly differentiated (P=2.111±0.333) expression levels using the IRS-Score method. Photomicrography showing Ki-67 expression levels in verrucous penile carcinoma (V) **(B)**, in well-differentiated penile carcinoma (W) **(C)**, and in moderately differentiated penile carcinoma (M) **(D)**. **E.** Ki-67 expression levels are elevated in poorly differentiated penile carcinoma (P). **p*<0.05, ***p*<0.01,****p*<0.001. x 320.

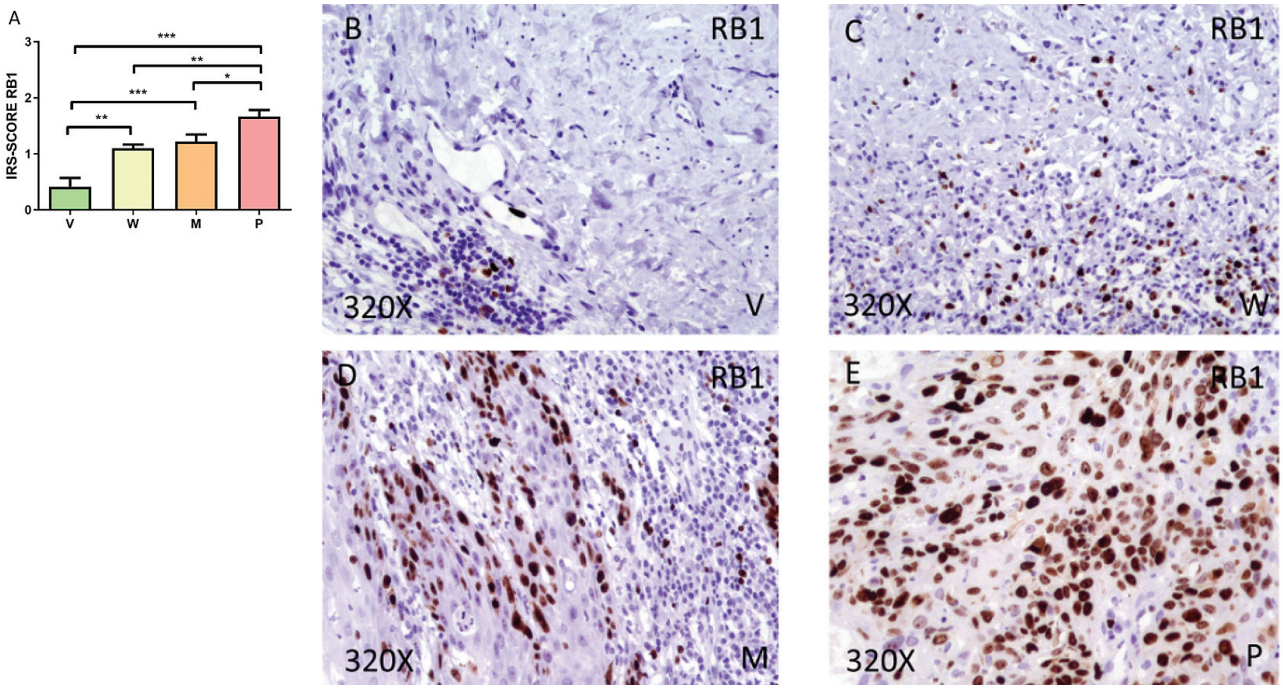

Fig. 3. A. The histological specimens were categorized into verrucous (V=0.417±0.376), well-differentiated (W=1.100±0.211), moderately differentiated (M=1.222±0.363), and poorly differentiated (P=1.667±0.354) expression levels using the IRS-Score method. Photomicrography showing the expression level of RB1 in verrucous penile carcinoma (V) **(B)**, in well-differentiated penile carcinoma (W) **(C)**, and in moderately differentiated penile carcinoma (M) **(D)**. **E.** RB1 expression levels are elevated in poorly differentiated penile carcinoma (P). **p*<0.05, ***p*<0.01, ****p*<0.001. x 320.

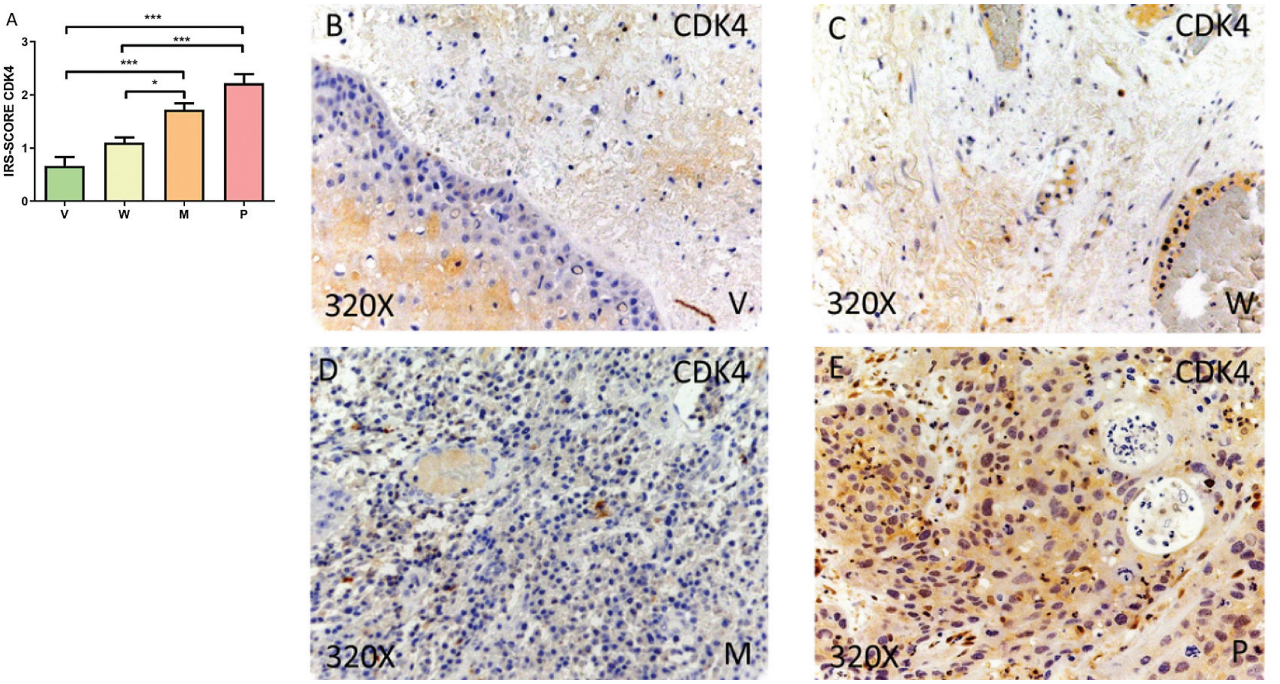

Fig. 4. A. The histological specimens were categorized into verrucous (V=0.667±0.408), well-differentiated (W=1.100±0.316), moderately differentiated (M=1.722±0.363), and poorly differentiated (P=2.222±0.507) expression levels using the IRS-Score method. Photomicrography showing the CDK4 expression level in verrucous penile carcinoma (V) **(B)**, in well-differentiated penile carcinoma (W) **(C)**, and in moderately differentiated penile carcinoma (M) **(D)**. **E.** CDK4 expression levels are elevated in poorly differentiated penile carcinoma (P). **p*<0.05, ***p*<0.01, ****p*<0.001. x 320.

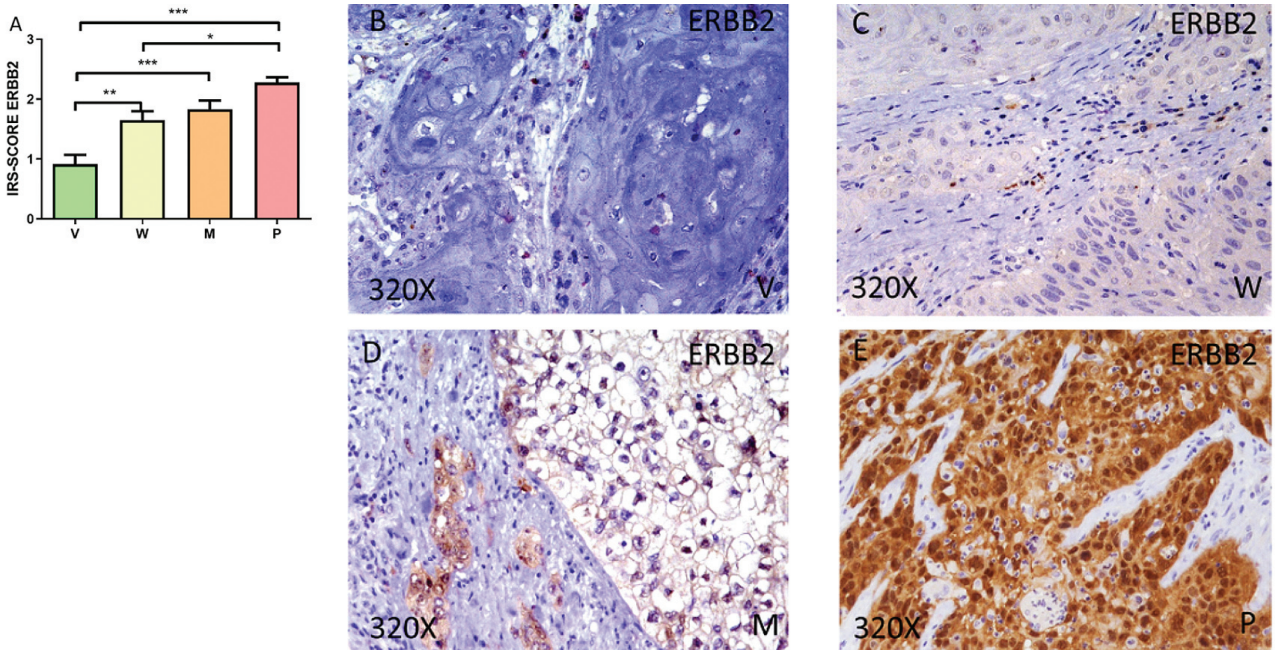

Fig. 5. A. The histological specimens were categorized into verrucous (V=0.833±0.258), well-differentiated (W=1.300±0.483), moderately differentiated (M=1.722±0.363), and poorly differentiated (P=2.111±0.417) expression levels using the IRS-Score method. Photomicrography showing the expression level of cyclin D1 in verrucous penile carcinoma (V) **(B)**, in well-differentiated penile carcinoma (W) **(C)**, and in moderately differentiated penile carcinoma (M) **(D)**. **E.** Photomicrography showing how the expression levels of cyclin D1 are elevated in poorly differentiated penile carcinoma (P). **p*<0.05, ***p*<0.01, ****p*<0.001. x 320.

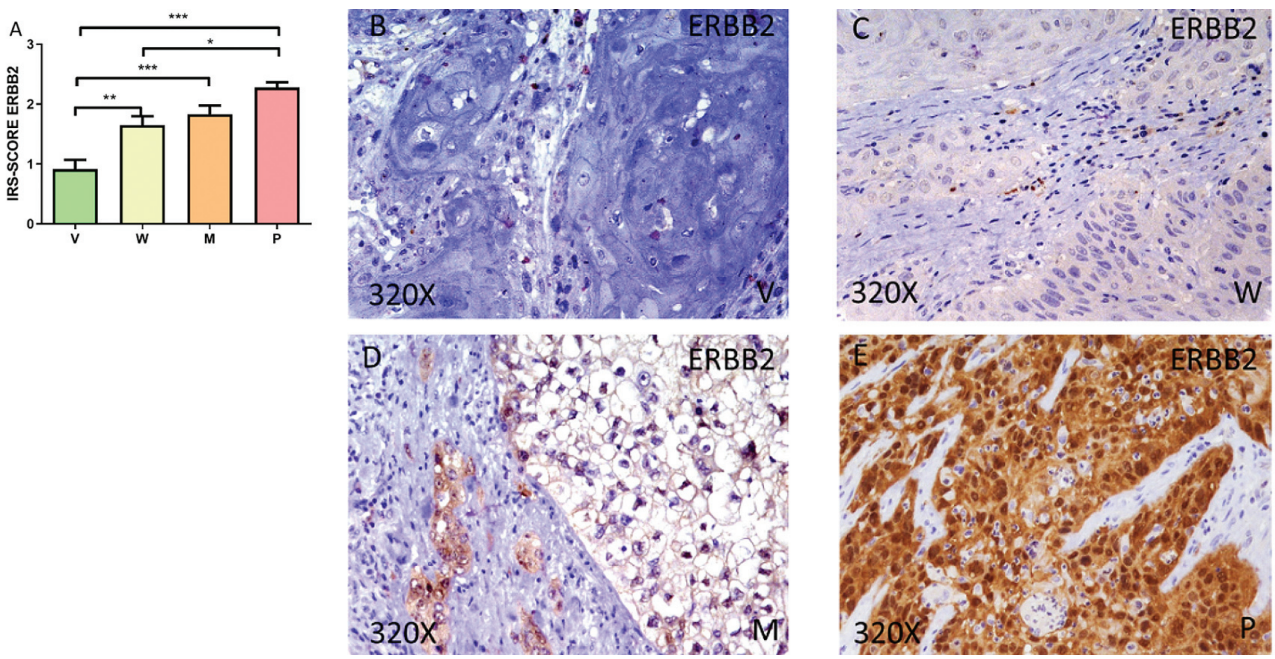

Fig. 6. A. Histological specimens were categorized into verrucous (V=0.917±0.376), well-differentiated (W=1.650±0.474), moderately differentiated (M=1.833±0.433), and poorly differentiated (P=2.278±0.264) expression levels using the IRS-Score method. Photomicrography showing ERBB2 expression level in verrucous penile carcinoma (V) **(B)**, in well-differentiated penile carcinoma (W) **(C)**, and in moderately differentiated penile carcinoma (M) **(D)**. **E.** ERBB2 expression levels are elevated in poorly differentiated penile carcinoma (P). **p*<0.05, ***p*<0.01, ****p*<0.001. x 320.

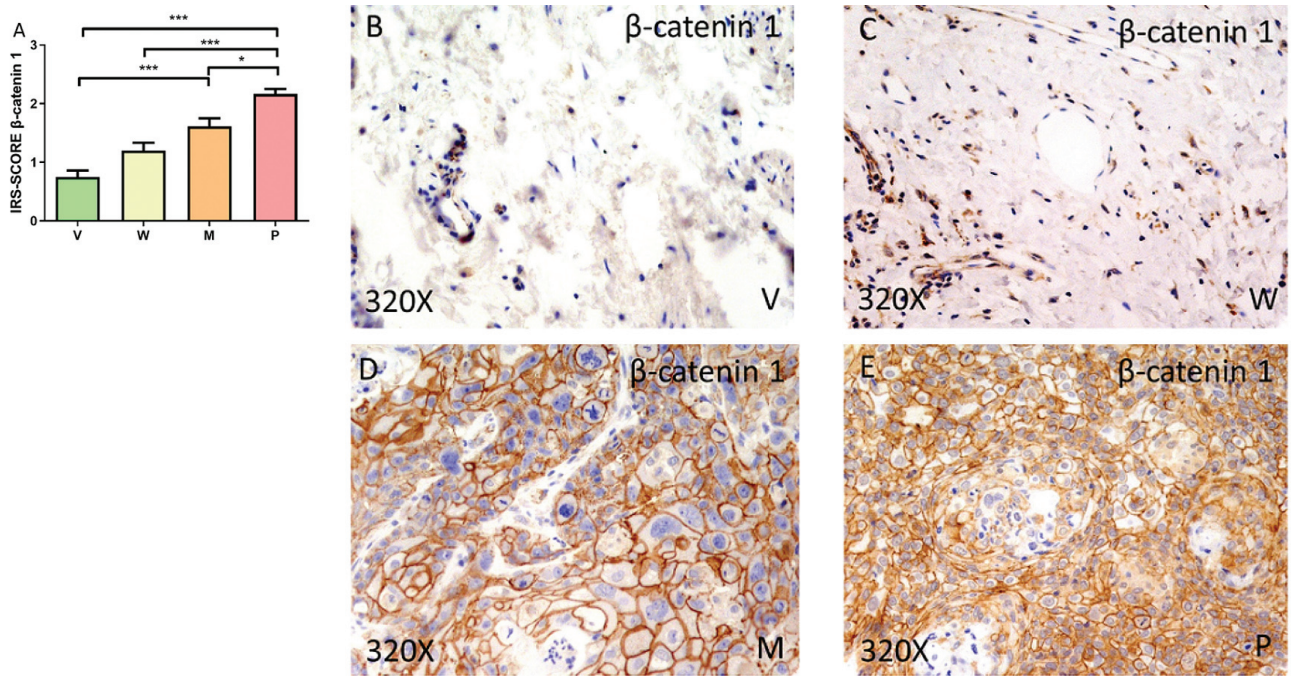

Fig. 7. A. Histological specimens were categorized into verrucous (V=0.750±0.274), well-differentiated (W=1.200±0.422), moderately differentiated (M=1.833±0.433), and poorly differentiated (P=2.167±0.250) expression levels using the IRS-Score method. Photomicrography showing the expression level of β-catenin 1 in verrucous penile carcinoma (V) **(B)**, in well-differentiated penile carcinoma (W) **(C)**, and in moderately differentiated penile carcinoma (M) **(D)**. **E.** It can be seen how the expression levels of β-catenin 1 are elevated in poorly differentiated penile carcinoma (P). **p*<0.05, ***p*<0.01, ****p*<0.001. x 320.

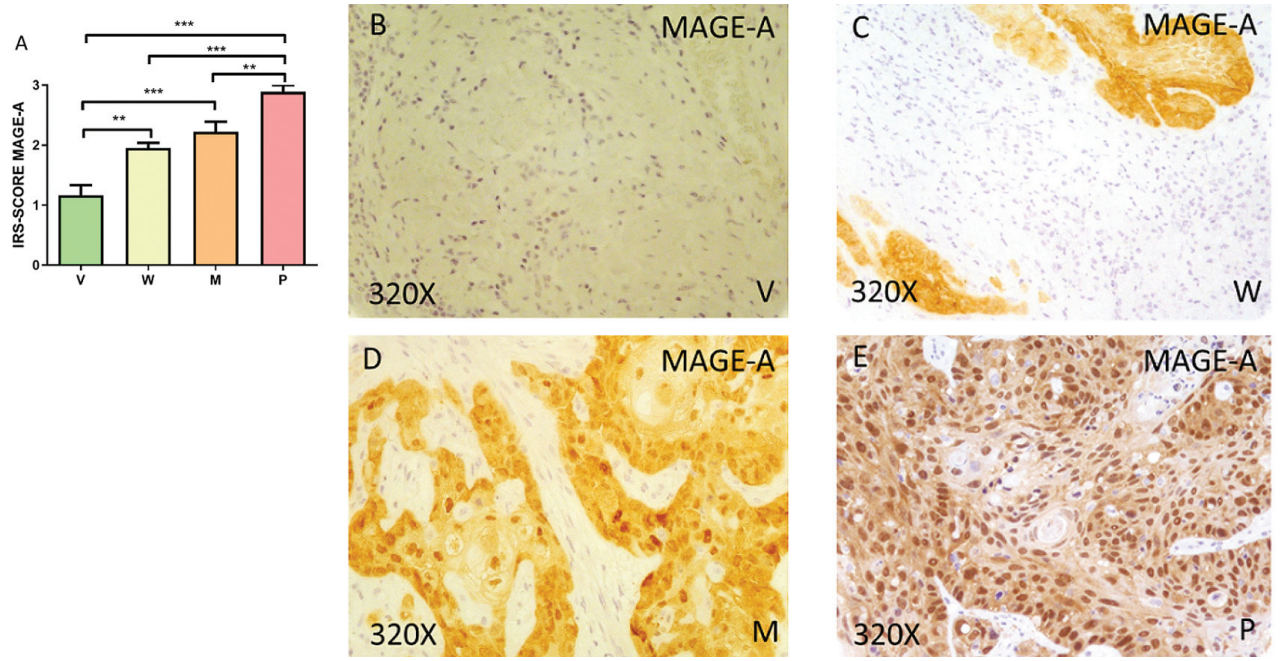

Fig. 8. A. The histological specimens were categorized into verrucous (V=1.167±0.408), well-differentiated (W=1.950±0.284), moderately differentiated (M=2.222±0.507), and poorly differentiated (P=2.889±0.333) expression levels using the IRS-Score method. Photomicrography showing the expression level of MAGE in verrucous penile carcinoma (V) **(B)**, in well-differentiated penile carcinoma (W) **(C)**, and in moderately differentiated penile carcinoma (M) **(D)**. **E.** It can be seen how the expression levels of MAGE-A are elevated in poorly differentiated penile carcinoma (P). **p*<0.05, ***p*<0.01, ****p*<0.001. x 320.

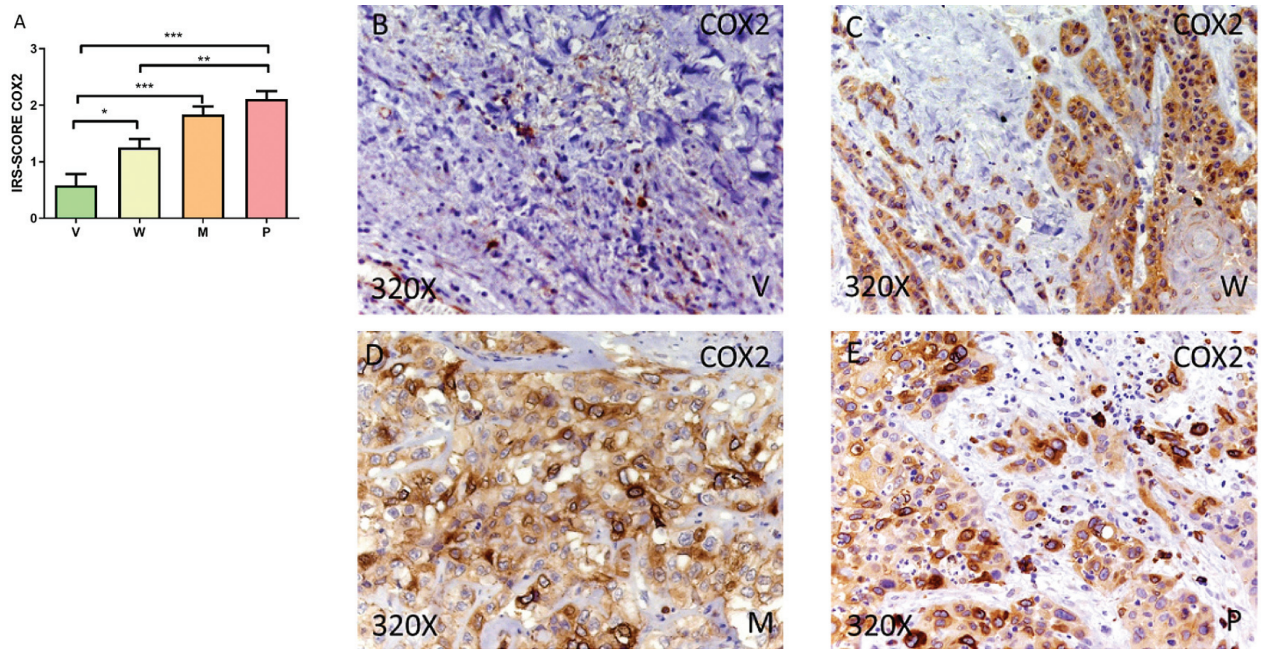

Fig. 9. A. Histological specimens were categorized into verrucous (V=0.583±0.492), well-differentiated (W=1.250±0.486), moderately differentiated (M=1.833±0.433), and poorly differentiated (P=2.111±0.417) expression levels using the IRS-Score method. Photomicrography showing the COX-2 expression level in verrucous penile carcinoma (V) **(B)**, in well-differentiated penile carcinoma (W) **(C)**, and in moderately differentiated penile carcinoma (M) **(D)**. **E.** It can be seen how COX-2 expression levels are elevated in poorly differentiated penile carcinoma (P). **p*<0.05, ***p*<0.01, ****p*<0.001. x 320.

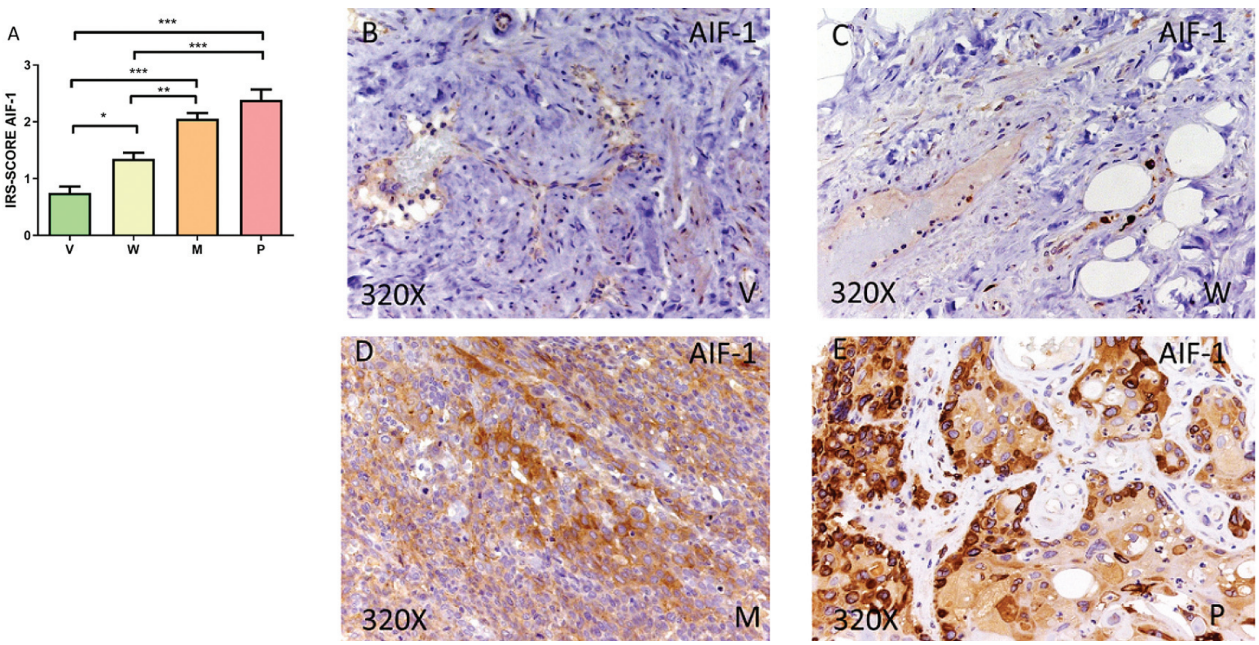

Fig. 10. A. The histological specimens were categorized into verrucous (V=0.750±0.274), well-differentiated (W=1.350±0.337), moderately differentiated (M=2.056±0.300), and poorly differentiated (P=2.389±0.546) expression levels using the IRS-Score method. Photomicrography showing the expression level of AIF-1 in verrucous penile carcinoma (V) **(B)**, in well-differentiated penile carcinoma (W) **(C)**, and in moderately differentiated penile carcinoma (M) **(D)**. **E.** AIF-1 expression levels are elevated in poorly differentiated penile carcinoma (P). **p*<0.05, ***p*<0.01, ****p*<0.001. x 320.

stages, it can be seen that the concentration of HAT-1 expression increases and is found in greater proportion in the P group (Fig. 12B-E).

Next, it was obtained that the expression of the proliferation marker ULK-1 intensifies as the disease worsened (Fig. 13A) (V=0.667±0.516; W=1.050±0.284; M=2.000±0.250; and P=2.611±0.417). In addition, in histological sections of the four stages, it can be seen

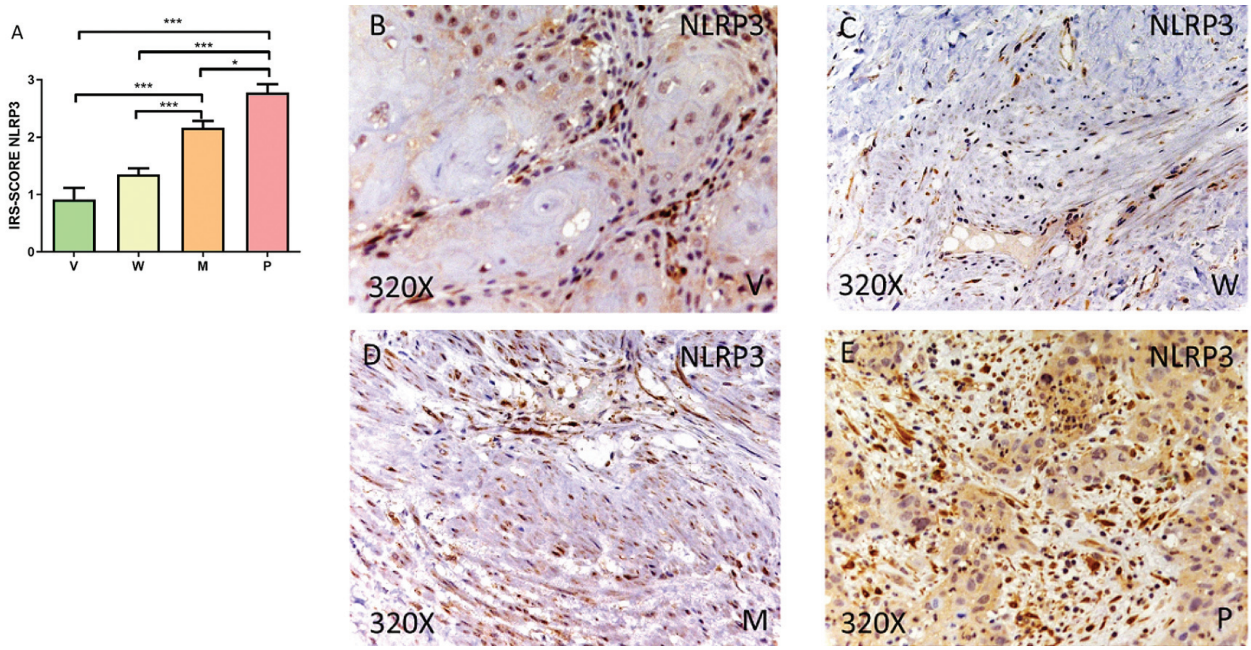

Fig. 11. A. Histological specimens were categorized into verrucous (V=0.917±0.492), well-differentiated (W=1.350±0.337), moderately differentiated (M=2.167±0.354), and poorly differentiated (P=2.778±0.441) expression levels using the IRS-Score method. Photomicrography showing the expression level of NLRP3 in verrucous penile carcinoma (V) **(B)**, in well-differentiated penile carcinoma (W) **(C)**, and in moderately differentiated penile carcinoma (M) **(D)**. **E.** NLRP3 expression levels are elevated in poorly differentiated penile carcinoma (P). **p*<0.05, ***p*<0.01, ****p*<0.001. x 320.

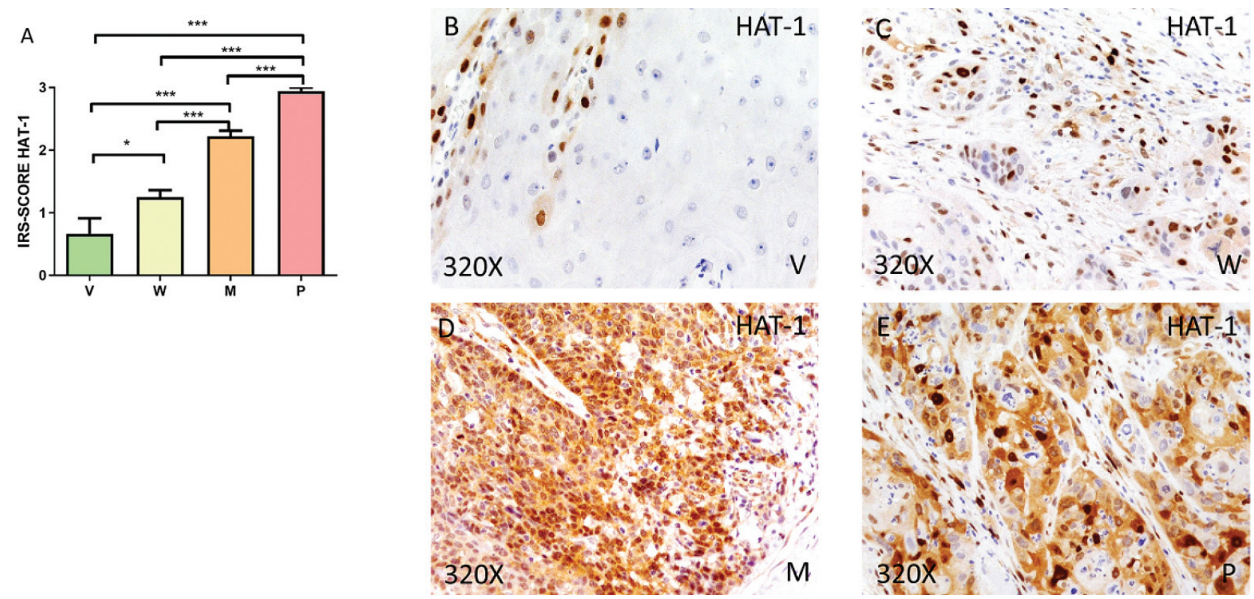

Fig. 12. A. The histological specimens were categorized into verrucous (V=0.667±0.606), well-differentiated (W=1.250±0.354), moderately differentiated (M=2.222±0.264), and poorly differentiated (P=2.944±0.167) expression levels using the IRS-Score method. Photomicrography showing the expression level of HAT-1 in verrucous penile carcinoma (V) **(B)**, in well-differentiated penile carcinoma (W) **(C)**, and in moderately differentiated penile carcinoma (M) **(D)**. **E.** HAT-1 expression levels are elevated in poorly differentiated penile carcinoma (P). **p*<0.05, ***p*<0.01, ****p*<0.001. x 320.

that the concentration of ULK-1 expression increases and is found in higher proportion in the P group (Fig. 13B-E).

Finally, the expression of biomarker ATG9A, related to cell proliferation, was observed. Said marker appears to increase as tumor progression worsens (Fig. 14A) (V=0.667±0.606; W=0.950±0.158; M=1.778±0.441; M=1.778±0.441). In addition, in histological sections of the four stages, it can be seen that the concentration of ATG9A expression increases and is found in greater

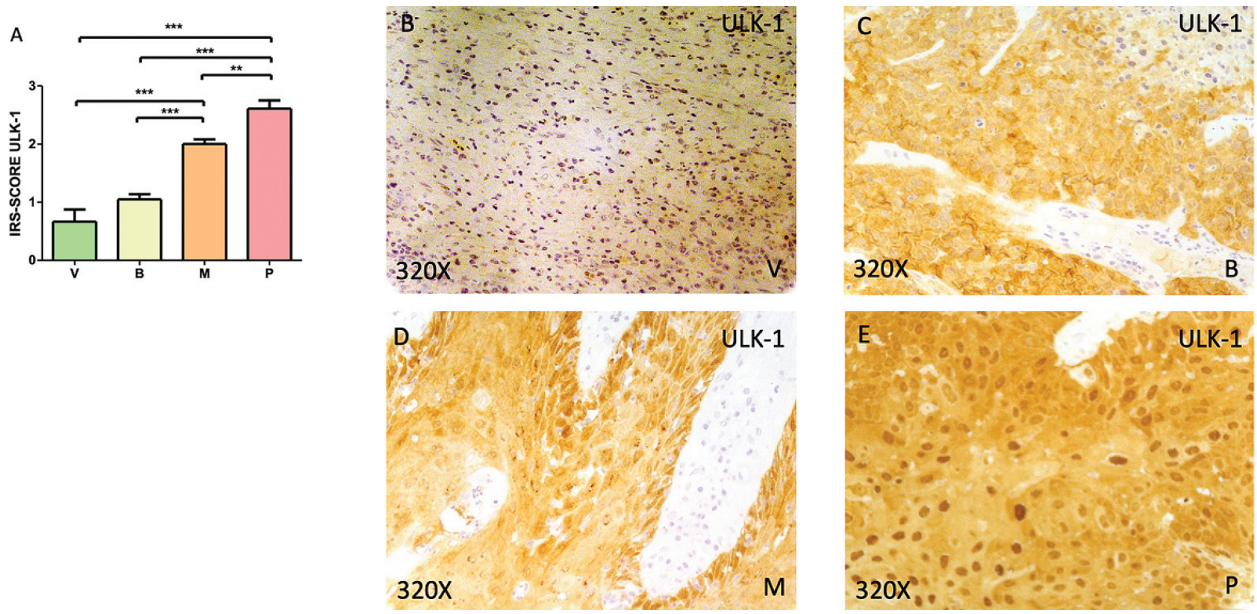

Fig. 13. A. Histological specimens were categorized into verrucous (V=0.667±0.516), well-differentiated (W=1.050±0.284), moderately differentiated (M=2.000±0.250), and poorly differentiated (P=2.611±0.417) expression levels using the IRS-Score method. Photomicrography showing the expression level of ULK-1 in verrucous penile carcinoma (V) **(B)**, in well-differentiated penile carcinoma (W) **(C)**, and in moderately differentiated penile carcinoma (M) **(D)**. **E.** ULK-1 expression levels are elevated in poorly differentiated penile carcinoma (P). **p*<0.05, ***p*<0.01, ****p*<0.001. x 320.

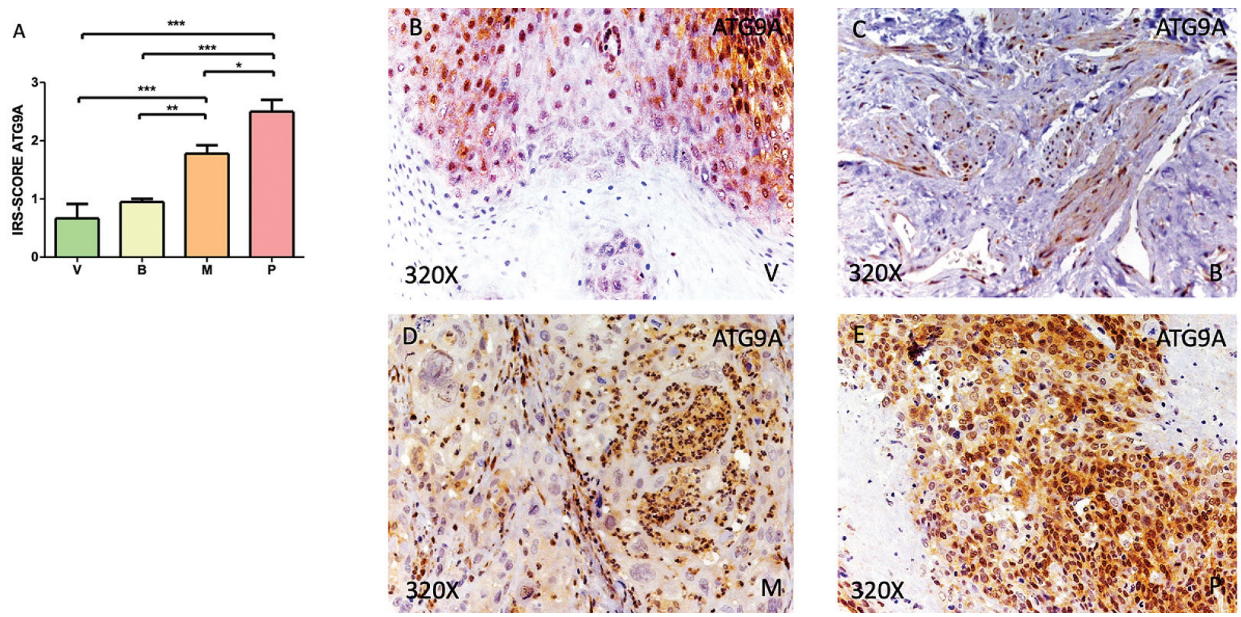

Fig. 14. A. Histological specimens were categorized into verrucous (V=0.667±0.606), well-differentiated (W=0.950±0.158), moderately differentiated (M=1.778±0.441), and poorly differentiated (M=1.778±0.441) expression levels using the IRS-Score method. Photomicrography showing the ATG9A expression level in verrucous penile carcinoma (V) **(B)**, in well-differentiated penile carcinoma (W) **(C)**, and in moderately differentiated penile carcinoma (M) **(D)**. **E.** ATG9A expression levels are elevated in poorly differentiated penile carcinoma (P). **p*<0.05, ***p*<0.01, ****p*<0.001. x 320.

proportion in the P group (Fig. 14B-E).

The data were corroborated with the Bonferroni test, as shown in Table 3.

Correlation analysis of the molecules studied found significant differences between different subtypes of penile squamous cell carcinoma

We performed a correlation analysis, expressed with the help of correlation matrices and heat maps (Figs. 15-19), to determine how the measured markers correlate according to their assigned IRS score from the histopathological point of view. Of note, looking at the heat maps by patient groups (penile cancer subtype), variations in expression patterns that change significantly from one group to another become very visible. However, performing the plot for the total penile cancer cohort has a different effect (Fig. 15); therefore,

Table 3. Bonferroni multiple comparison test of means between all penile cancer subtypes with all biomarkers used in the study.

Bonferroni multiple comparison test	Mean differences	t	Significant $p<0.05$?	Summary	95% confidence interval of mean differences
IRS-4					
V vs. W	-0.7333	4.253	Yes	**	-1.220 to -0.2463
V vs. M	-1.139	6.472	Yes	***	-1.636 to -0.6418
V vs. P	-1.972	11.21	Yes	***	-2.469 to -1.475
W vs. M	-0.4056	2.644	No	ns	-0.8389 to 0.02778
W vs. P	-1.239	8.076	Yes	***	-1.672 to -0.8056
M vs. P	-0.833	5.294	Yes	***	-1.278 to -0.3887
Ki-67					
V vs. W	-0.4667	2.461	No	ns	-1.002 to 0.06891
V vs. M	-0.8611	4.450	Yes	***	-1.408 to -0.3145
V vs. P	-1.528	7.895	Yes	***	-2.074 to -0.9812
W vs. M	-0.3944	2.338	No	ns	-0.8710 to 0.08209
W vs. P	-1.061	6.290	Yes	***	-1.538 to -0.5846
M vs. P	-0.6667	3.852	Yes	**	-1.156 to -0.1778
RB-1					
V vs. W	-0.6833	4.075	Yes	**	-1.157 to -0.2096
V vs. M	-0.8056	4.706	Yes	***	-1.289 to -0.3221
V vs. P	-1.250	7.303	Yes	***	-1.733 to -0.7665
W vs. M	-0.1222	0.8191	No	ns	-0.5437 to 0.2993
W vs. P	-0.5667	3.798	Yes	**	-0.9881 to -0.1452
M vs. P	-0.4444	2.903	Yes	*	-0.8769 to -0.01202
CDK4					
V vs. W	-0.4333	2.088	No	ns	-1.019 to 0.1528
V vs. M	-1.056	4.984	Yes	***	-1.654 to -0.4573
V vs. P	-1.556	7.345	Yes	***	-2.154 to -0.9573
W vs. M	-0.6222	3.370	Yes	*	-1.144 to -0.1007
W vs. P	-1.122	6.078	Yes	***	-1.644 to -0.6007
M vs. P	-0.5000	2.639	No	ns	-1.035 to 0.03509
CYCLIN-D1					
V vs. W	-0.4667	2.241	No	ns	-1.055 to 0.1215
V vs. M	-0.8889	4.183	Yes	**	-1.489 to -0.2886
V vs. P	-1.278	6.013	Yes	***	-1.878 to -0.6775
W vs. M	-0.4222	2.279	No	ns	-0.9456 to 0.1011
W vs. P	-0.8111	4.378	Yes	***	-1.334 to -0.2878
M vs. P	-0.3889	2.046	No	ns	-0.9258 to 0.1480
ERBB2					
V vs. W	-0.7333	3.554	Yes	**	-1.316 to -0.1505
V vs. M	-0.9167	4.353	Yes	***	-1.511 to -0.3219
V vs. P	-1.361	6.464	Yes	***	-1.956 to -0.7663
W vs. M	-0.1833	0.9987	No	ns	-0.7019 to 0.3352
W vs. P	-0.6278	3.420	Yes	*	-1.146 to -0.1092
M vs. P	-0.4444	2.360	No	ns	-0.9765 to 0.08756
β-CATENIN 1					
V vs. W	-0.4500	2.428	No	ns	-0.9735 to 0.07349
V vs. M	-0.8611	4.553	Yes	***	-1.395 to -0.3268
V vs. P	-1.417	7.490	Yes	***	-1.951 to -0.8824
W vs. M	-0.4111	2.493	No	ns	-0.8769 to 0.05466
W vs. P	-0.9667	5.862	Yes	***	-1.432 to -0.5009
M vs. P	-0.5556	3.284	Yes	*	-1.033 to -0.07768

the separation between groups allowed us to obtain a broader idea of the different expression patterns in each disease subtype (Figs. 16-19). In the first instance, the joint correlation analysis without patient classification exhibits a strong correlation between all variables (Fig. 15).

By observing a significantly strong correlation, we could gain insight into the functional relationships between the protein markers studied or their influence on each other's expression levels. This means that there could be patterns of co-expression between markers, which would allow us to understand the course of the disease in each group of patients. Subsequently, we carried out a correlation analysis in each group of patients to see how the relationships between markers vary and, thus, how their protein expression patterns converge or diverge.

Starting the correlation analyses with patients

Table 3. (Continued).

Bonferroni multiple comparison test	Mean differences	t	Significant $p<0.05$?	Summary	95% confidence interval of mean differences
MAGE-A					
V vs. W	-0.7833	3.915	Yes	**	-1.348 to -0.2182
V vs. M	-1.056	5.170	Yes	***	-1.632 to -0.4788
V vs. P	-1.722	8.435	Yes	***	-2.299 to -1.145
W vs. M	-0.2722	1.529	No	ns	-0.7750 to 0.2306
W vs. P	-0.9389	5.274	Yes	***	-1.442 to -0.4361
M vs. P	-0.6667	3.650	Yes	**	-1.183 to -0.1508
COX-2					
V vs. W	-0.6667	2.835	Yes	*	-1.331 to -0.002365
V vs. M	-1.250	5.208	Yes	***	-1.928 to -0.5720
V vs. P	-1.528	6.365	Yes	***	-2.206 to -0.8498
W vs. M	-0.5833	2.788	No	ns	-1.174 to 0.007733
W vs. P	-0.8611	4.115	Yes	**	-1.452 to -0.2700
M vs. P	-0.2778	1.294	No	ns	-0.8842 to 0.3286
AIF-1					
V vs. W	-0.6000	2.996	Yes	*	-1.166 to -0.03437
V vs. M	-1.306	6.388	Yes	***	-1.883 to -0.7283
V vs. P	-1.639	8.019	Yes	***	-2.216 to -1.062
W vs. M	-0.7056	3.960	Yes	**	-1.209 to -0.2023
W vs. P	-1.039	5.831	Yes	***	-1.542 to -0.5356
M vs. P	-0.3333	1.823	No	ns	-0.8497 to 0.1830
NLRP3					
V vs. W	-0.4333	2.100	No	ns	-1.016 to 0.1495
V vs. M	-1.250	5.936	Yes	***	-1.845 to -0.6552
V vs. P	-1.861	8.838	Yes	***	-2.456 to -1.266
W vs. M	-0.8167	4.449	Yes	***	-1.335 to -0.2981
W vs. P	-1.428	7.778	Yes	***	-1.946 to -0.9092
M vs. P	-0.6111	3.245	Yes	*	-1.143 to -0.07910
HAT-1					
V vs. W	-0.5833	3.201	Yes	*	-1.098 to -0.06858
V vs. M	-1.556	8.363	Yes	***	-2.081 to -1.030
V vs. P	-2.278	12.25	Yes	***	-2.803 to -1.752
W vs. M	-0.9722	5.996	Yes	***	-1.430 to -0.5142
W vs. P	-1.694	10.45	Yes	***	-2.152 to -1.236
M vs. P	-0.7222	4.341	Yes	***	-1.192 to -0.2523
ULK-1					
V vs. W	-0.3833	2.046	No	ns	-0.9124 to 0.1458
V vs. M	-1.333	6.974	Yes	***	-1.873 to -0.7933
V vs. P	-1.944	10.17	Yes	***	-2.484 to -1.404
W vs. M	-0.9500	5.700	Yes	***	-1.421 to -0.4792
W vs. P	-1.561	9.367	Yes	***	-2.032 to -1.090
M vs. P	-0.6111	3.574	Yes	**	-1.094 to -0.1281
ATG9A					
V vs. W	-0.2833	1.169	No	ns	-0.9682 to 0.4016
V vs. M	-1.111	4.490	Yes	***	-1.810 to -0.4121
V vs. P	-1.833	7.408	Yes	***	-2.532 to -1.134
W vs. M	-0.8278	3.837	Yes	**	-1.437 to -0.2184
W vs. P	-1.550	7.185	Yes	***	-2.159 to -0.9406
M vs. P	-0.7222	3.263	Yes	*	-1.347 to -0.09701

stratified by disease group, we see more detailed differences in protein expression patterns. In V penile cancer (Fig. 16), we observe a moderately strong positive correlation (p<0.01) between cyclin D1, HAT-1, and AIF-1 with COX2; also, with the same degree of significance (p<0.01) cyclin D1 correlated with Ki-67. We see a significant positive correlation (p<0.05) between ATG9A with HAT-1, AIF-1, and ULK-1. NLRP3 establishes the same relationship with CDK4, as well as AIF-1 with HAT-1, HAT-1 with cyclin D1, cyclin D1 with RB1, COX2 with IRS4 and RB1, RB1 with Ki-67, and finally, Ki-67 with IRS4. We also found several pairs of variables without any linear relationship (in white, Fig. 16).

In the correlations with W penile cancer (Fig. 17), we observed a moderately significant positive correlation (p<0.01) between RB1 with Ki-67, MAGE-A with IRS4, and AIF-1 with HAT-1. We also found significant directly proportional correlations for ATG9A with Ki-67 and ULK-1; ULK-1 with HAT-1, AIF-1, and NLRP3; NLRP3 with AIF-1; HAT-1 with COX2; MAGE-A with Ki-67; β-catenin with COX2 and CDK4; ERBB2 with IRS4 and COX2; RB1 with Ki-67; and IRS4 with Ki-67 and COX2. Alignment between some pairs of variables was also observed (in white, Fig. 17).

Establishing linearity relationships in M penile cancer (Fig. 18), a perfect (p<0.001) and positive (1) correlation was observed between cyclin D1 and CDK4, in addition to a positive and highly significant (p<0.001) correlation between MAGE-A and IRS4. Alternatively, there is a moderately significant positive correlation (p<0.01) between ERBB2 and Ki-67 with IRS4; also, AIF-1 and MAGE-A with Ki-67; ULK-1 with AIF-1; and ATG9A with ULK-1. In addition, there is positive collinearity and statistical significance (p<0.05) for ERBB2 with Ki-67 and COX2; MAGE-A with ERBB2; HAT-1 with Ki-67; AIF-1 with MAGE-A; ULK-1 with NLRP3; and ATG9 with NLRP3. Likewise, there was no linear relationship between several pairs of variables, denoting a different disease pattern from the previous ones (in white, Fig. 18).

Lastly, in the correlation analysis in the case of patients with P penile cancer (Fig. 19), the color pattern in the heat map can be seen to change notably, given that here we move on to variables that are negatively correlated. We first observe a positive correlation and high significance (p<0.001) between cyclin D1 and β-catenin with CDK4; in addition to NLRP3 and ULK-1 with ATG9A. With a moderately high significance (p<0.01), we found positive collinearity between cyclin D1 with COX2 and ULK-1 with NLRP3. With statistical significance, we also observed positive collinearity between RB1 with IRS4; CDK4 with COX2; ERBB2 with Ki67 and the same with RB1; β-catenin with COX2 and with cyclin D1; MAGE-A with Ki-67 and RB1; and finally, between ULK-1 and ATG9A with AIF-1. Ultimately, a negative linear relationship was also established between AIF-1 and CDK4. There were only

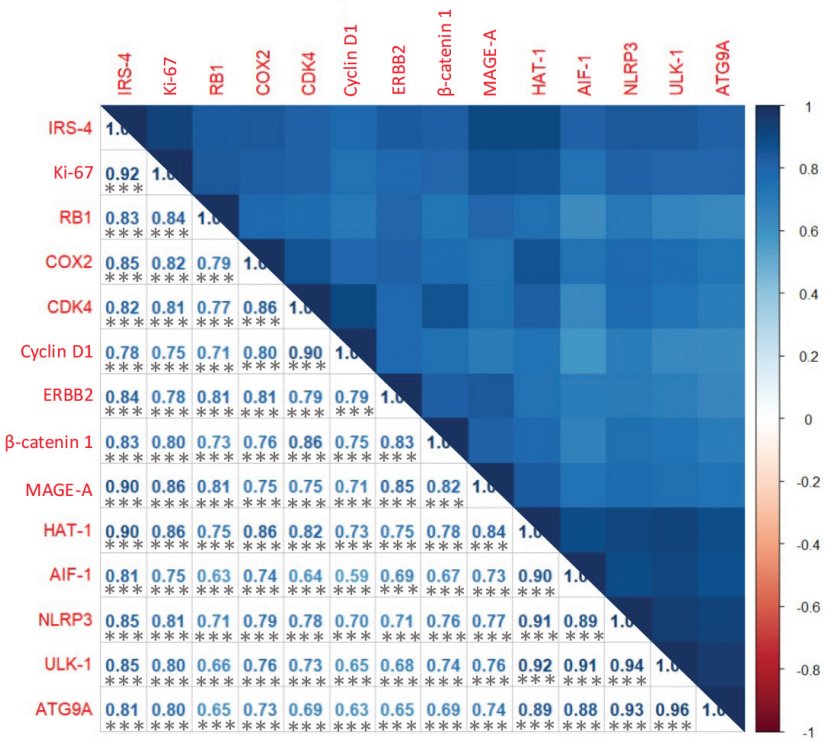

Fig. 15. Correlation of variables considering the complete cohort (without classification). Correlation matrix + heat map of the molecular markers included in the study. Note: The graph shows the Pearson coefficients with their corresponding degrees of significance. The diagonal represents the perfect correlation (1), that of each protein with itself. The warm colors represent negative correlations (-1.0) or inversely proportional in this specific case, while cold colors represent positive correlations (0.1) or directly proportional in this specific case. *p<0.05, **p<0.01, ***p<0.001.

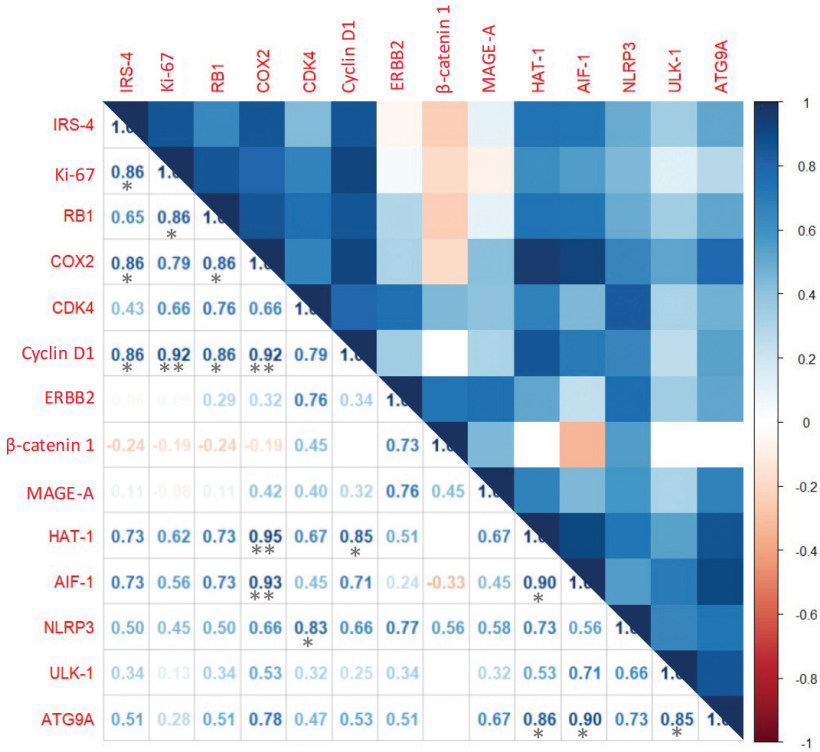

Fig. 16. Correlation of variables in the "verrucous" penile cancer group. Correlation matrix + heat map of the molecular markers included in the study. Note: The graph shows the Pearson coefficients with their corresponding degrees of significance. The diagonal represents the perfect correlation (1), that of each protein with itself. The warm colors represent negative correlations (-1.0) or inversely proportional in this specific case, while cold colors represent positive correlations (0.1) or directly proportional in this specific case. *p<0.05, **p<0.01, ***p<0.001.

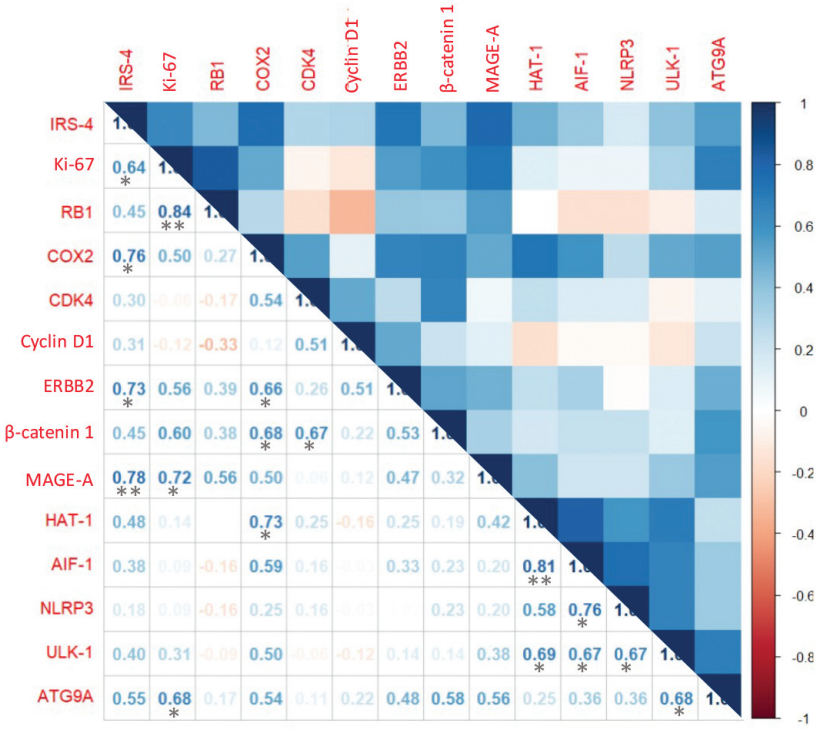

Fig. 17. Correlation of variables in the "well-differentiated" penile cancer group. Correlation matrix + heat map of the molecular markers included in the study. Note: The graph shows the Pearson coefficients with their corresponding degrees of significance. The diagonal represents the perfect correlation (1), that of each protein with itself. The warm colors represent negative correlations (-1.0) or inversely proportional in this specific case, while cold colors represent positive correlations (0.1) or directly proportional in this specific case. *p<0.05, **p<0.01, ***p<0.001.

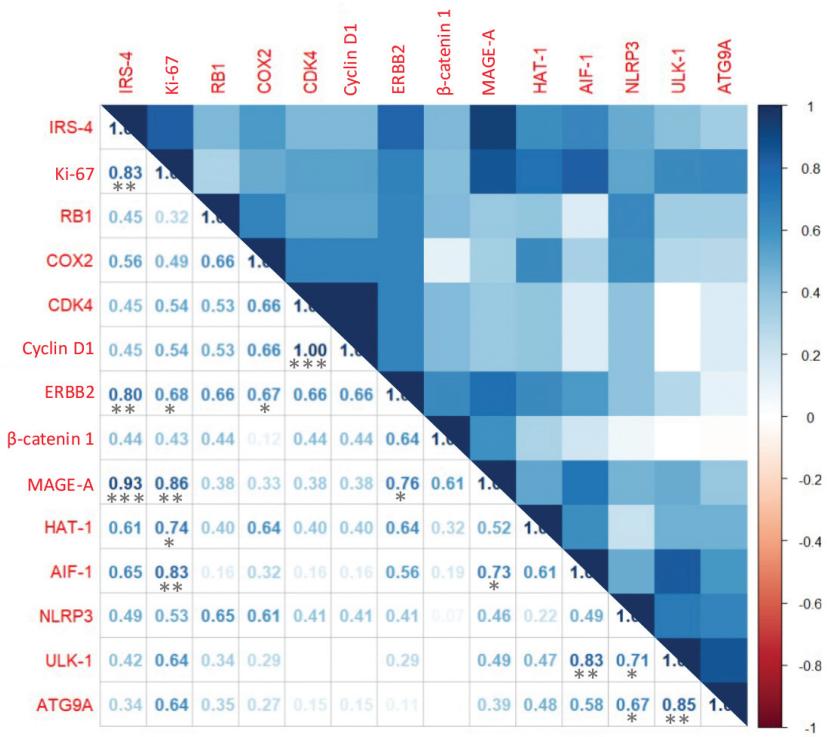

Fig. 18. Correlation of variables in the "moderately differentiated" penile cancer group. Correlation matrix + heat map of the molecular markers included in the study. In this case, a perfect correlation (1) is found between CDK4 and cyclin D1. Near-perfect correlation (0.93) is found between MAGE and IRS4. Note: The graph shows the Pearson coefficients with their corresponding degrees of significance. The diagonal represents the perfect correlation (1), that of each protein with itself. The warm colors represent negative correlations (-1.0) or inversely proportional in this specific case, while cold colors represent positive correlations (0.1) or directly proportional in this specific case. *p<0.05, **p<0.01, ***p<0.001.

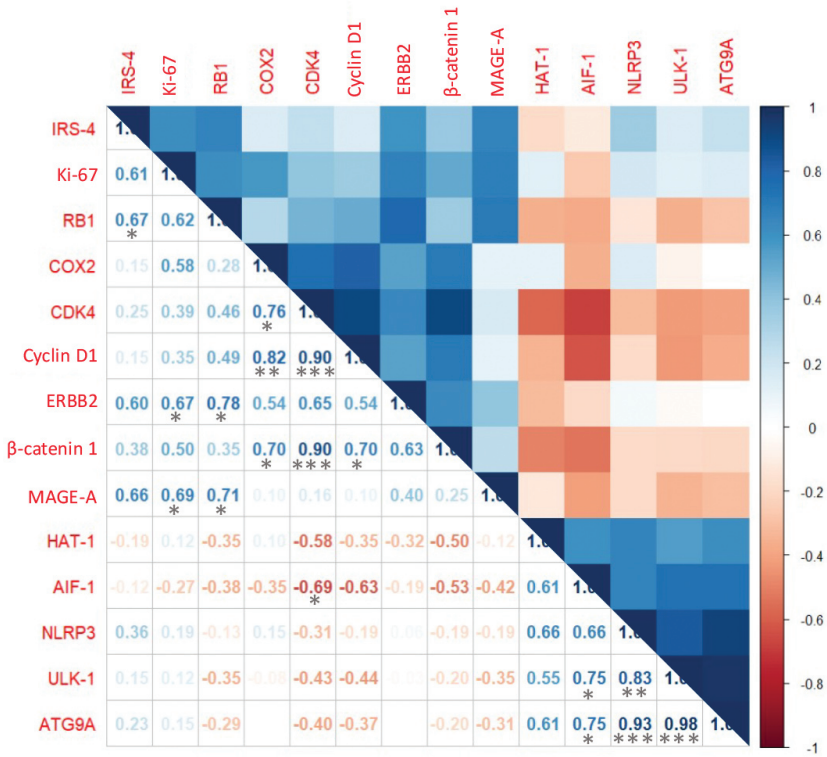

Fig. 19. Correlation of variables in the "poorly differentiated" penile cancer group. Correlation matrix + heat map of the molecular markers included in the study. An almost perfect correlation is found between CDK4 and cyclin D1 (0.90) and CDK4 and B-catenin 1 (0.90). Also, ATG9A with NLRP3 (0.93) and ULK-1 (0.98). Note: The graph shows the Pearson coefficients with their corresponding degrees of significance. The diagonal represents the perfect correlation (1), of each protein with itself. The warm colors represent negative correlations (-1.0) or inversely proportional in this specific case, while cold colors represent positive correlations (0.1) or directly proportional ones. *p<0.05, **p<0.01, ***p<0.001.

alignments between ATG9A with COX2 and ERBB2 (in white, Fig. 19).

Odds ratio estimation: Principal Component Analysis (PCA) and Multinomial Logistic Regression (MLR).

PCA (*Supplementary Materials S1*, *S2*, and *S3*) allowed us to evaluate the association between the combined protein expression profile (reducing dimensionality in the two PCs) and group classification while controlling for IRS scores. The RLM model provided the assigned odds ratios for the patient group (Table 4).

With the results obtained from the multinomial linear regression model, we can interpret the coefficients as the odds of transitioning of each patient group to the reference ("V") group. Positive coefficients indicate an increase in the probability of transitioning to the corresponding group, while negative coefficients indicate a decrease.

For the "W" group:

- The intercept of 9.612349 represents the baseline odds of transitioning to the "W" group compared to the reference group ("V").
- The coefficient for PC1 (2.831983) indicates that a higher value of the first principal component (PC1) increases the probability of transitioning to the "W" group, as indicated by the positive value.
- The coefficient for Pc2 (-3.405405) implies that a higher value of the second principal component (PC2) decreases the likelihood of transitioning to the "W" group, as shown by the negative coefficient.

For the "M" group:

- The intercept of 16.904714 reflects the baseline odds for transitioning to the "M" group compared to the reference group ("V").
- The coefficient for PC1 (23.757308) suggests that an increase in PC1 significantly raises the probability of transitioning to the "M" group.
- The coefficient PC2 (8.387335) indicates that a higher value of PC2 also increases the probability of transitioning to this group, as denoted by the positive coefficient.

For the "P" group:

- The intercept of 12.241944 denotes the baseline odds of transitioning to the "P" group compared to the reference group ("V").
- The coefficient for PC1 (25.472907) shows that an increase in PC1 strongly elevates the likelihood of transitioning to the "P" group.
- The coefficient for PC2 (8.565876) also indicates that a rise in PC2 positively impacts the probability of transitioning to this group.

Discussion

In the present work we have focused on evaluating, using immunohistochemical techniques, the protein expression of a series of biomarkers involved in the regulation of growth and cell cycle, inflammation, autophagy, and epigenetics, in different types of PSCCs. Our results show that there is a differential expression of a wide set of regulatory molecules of these processes according to the degree of cell differentiation. This could indicate the existence of different carcinogenic mechanisms depending on the degree of differentiation. However, it is known that the degree of differentiation represents an important prognostic value in penile squamous carcinoma, with P tumors having a worse prognosis, followed by M and W, while V tumors have a better prognosis (Velazquez et al., 2008; Chaux et al., 2009). Thus, the proteins we have analyzed could have potential prognostic value as they are more expressed in tumors with a worse prognosis, although further research is required to confirm this hypothesis. Future lines of research could assess the validity of these markers as potential therapeutic targets in aggressive variants of this type of cancer, alongside other well-established molecules, such as PD-L1 or microsatellite instability (Montella et al., 2022). Nevertheless, the correlogram also shows interesting and significant differences in the molecular expression patterns of the different proteins included, thus showing distinctive biological patterns related to the degree of cell differentiation. The odds ratio estimation also suggests that these variables could potentially have an important impact on the differentiation of PSCC groups. The different molecules and cellular processes considered in the present study, as well as the interpretation of the statistical analyses performed, will be detailed below.

The study acknowledges certain limitations that must be considered when interpreting the results. One significant limitation is the relatively small number of cases in each differentiation group, which can affect the

Table 4. Odds ratios estimate for each group compared to the verrucous type, *p* value of model: 1.277571e-15.

Group	Odds ratio (coefficients±SD)		
	Intercept	PC1	PC2
W	9.612349±7.065516	2.831983±2.065565	-3.405405±3.467105
M	16.904714±19.467447	23.757308±40.527181	8.387335±31.798641
P	12.241955±19.615269	25.472907±40.535195	8.565876±31.804789

In interpreting the principal component coefficients, we considered the overall patterns of variability in the data (captured by PC1 and PC2), which are related to the outcome of interest (in this case, the patient group).

statistical power and generalizability of the findings. Also, the overall number of cases included in the study may be insufficient to draw robust conclusions about the role of specific biomarkers in penile carcinoma. The limited availability of data on these biomarkers, particularly in rare cancers like penile carcinoma, poses challenges for developing a comprehensive understanding of their prognostic value. Future studies with larger sample sizes and a more balanced representation of differentiation subtypes are necessary to confirm these preliminary findings and to strengthen the reliability of biomarkers as indicators of prognosis.

Histopathological markers of proliferation and cell cycle in penile cancer

Cancer cells are characterized by their ability to maintain chronic proliferation due to an uncontrolled cell cycle (Feitelson et al., 2015). This process is influenced by growth factors interacting with cell receptors, triggering signaling pathways that control cell growth and division (Yun et al., 2010; Hanahan and Weinberg, 2011). Tumors can enhance proliferation through autocrine and paracrine stimulation but mutations in cancer disrupt cell cycle regulation, allowing continuous division (Visconti et al., 2016; Matthews et al., 2021).

This study identified markers linked to proliferation in PSCCs, including IRS-4, Ki-67, RB1, CDK4, Cyclin D1, ERBB2, ß-catenin, and MAGE. These markers were significantly elevated in more aggressive tumors (P and M stages).

First, we found that IRS-4, an adaptor protein, less studied in comparison to other IRS family members, showed increased expression in aggressive penile carcinoma (P and M states. IRS-4 overexpression, observed in various other cancers, suggests its potential role in activating oncogenes through pathways like PI3K/Akt and MAPK, making it a promising biomarker and therapeutic target for more aggressive penile cancers (Shaw, 2011; Hao et al., 2021; Kuasne et al., 2021; Thomas et al., 2021b; White and Kahn, 2021; Guijarro et al., 2023).

Next, we saw that the expression of biomarker Ki-67, known as a marker of cell proliferation, showed higher expression in less differentiated carcinomas (P, M, and W). Its role as a prognostic biomarker in penile carcinoma remains controversial as studies have linked it to lymph node metastasis but not necessarily to survival outcomes (Gerdes et al., 1983; Berdjis et al., 2005; Urruticoechea et al., 2005; Guimarães et al., 2007; Stankiewicz et al., 2012; Cuylen et al., 2016; Sobecki et al., 2016; Sun et al., 2017; Miller et al., 2018; Mehdi et al., 2023).

We also analyzed Cyclin D1/CDK4/6 and RB1 as cell cycle regulators that were more expressed in aggressive tumors. Cyclin D1-CDK4 complexes regulate the G1-to-S phase transition in the cell cycle. Increased expression of these proteins in less differentiated penile carcinomas suggests their potential as biomarkers and therapeutic targets (Paternot et al., 2010; Suryadinata et al., 2010; Baker and Reddy, 2012; Mirzaa et al., 2014; McDaniel et al., 2015; Hamilton and Infante, 2016; Fenner et al., 2018; Ortiz et al., 2021).

In contrast, RB1 acts as a tumor suppressor regulating cell cycle progression, it is more expressed in less differentiated tumors. While alterations in RB1 have been observed in PSCC, its prognostic value remains to be confirmed (Chinnam and Goodrich, 2011; Reuschenbach et al., 2012; Indovina et al., 2015; Marchi et al., 2017; Ren and Gu, 2017; Berry et al., 2019; Huang et al., 2019; Macedo et al., 2020; da Silva et al., 2022; Ortega et al., 2022b; Xie et al., 2022; Liu et al., 2023).

Another biomarker we studied was ERBB2, this receptor plays a role in carcinogenesis by activating pathways like PI3K/Akt/mTOR. ERBB2 overexpression has been linked to the progression of various cancers, including penile carcinoma (Yarden and Pines, 2012; Arteaga and Engelman, 2014; Miller et al., 2019; Roskoski, 2019; Padayachee et al., 2020; Zhang et al., 2021; Zhu et al., 2021; Tan et al., 2023).

Also, we studied the role of β-catenin, a key transcription factor in the Wnt pathway. β-catenin is associated with P tumors. Its role in penile carcinoma development suggests it may be a prognostic biomarker. (Niehrs and Acebron, 2012; Cruciat and Niehrs, 2013; Arya et al., 2015; Perugorria et al., 2019; Yu et al., 2021; Liu et al., 2022).

Finally, the MAGE-A marker forms part of the MAGE protein family and is implicated in cancer progression. MAGE proteins interact with E3 ligases to regulate protein ubiquitination, making them potential biomarkers and therapeutic targets in PSCC (Doyle et al., 2010; Miranda, 2010; Hao et al., 2013; Weon and Potts, 2015; Hagiwara et al., 2016; Newman et al., 2016; De Donato et al., 2017).

Further studies are needed to validate the role of these markers as therapeutic targets and prognostic tools in PSCC.

Histopathological markers of inflammation in penile cancer

Inflammation has an important role in cancer development and progression by supporting key cancer hallmarks, such as cell proliferation and mutagenesis (Singh et al., 2019). Tumor and stromal cells create an inflammatory tumor microenvironment (ITM), which interacts with immune cells and promotes tumor growth (Denk and Greten, 2022). This ITM is driven by mechanisms like oncogene activation, inactivation of tumor suppressors, oxidative stress, and hypoxia (Greten and Grivennikov, 2019). Chronic inflammation due to factors like obesity, autoimmune conditions, and HPV infections is also linked to increased cancer risk, including penile cancer (Greten and Grivennikov, 2019). Evidence suggests inflammation has a dual role in

cancer, promoting progression while also serving as a potential tumor-suppressive mechanism (Protzel and Spiess, 2013; Engelsgjerd and LaGrange, 2022; Janicic et al., 2023). Biomarkers of inflammation, such as COX-2, NLPR3, and AIF-1, are emerging as key elements in both the development and prognosis of cancers, including penile cancer.

In penile cancer, systemic and local inflammation, driven by factors like balanitis and phimosis, contributes to tumor progression (Douglawi and Masterson, 2017). Markers like IL-1A, IL-6, interferon-gamma, and COX-2 are upregulated in penile cancer (Czajkowski et al., 2023), with COX-2 and its metabolite PGE2 promoting angiogenesis, proliferation, and metastasis (Hashemi Goradel et al., 2019). COX-2 overexpression has been linked to poor outcomes in various cancers (Ortega et al., 2022b; Purnama et al., 2023), and our findings show higher COX-2 levels in more aggressive penile cancer subtypes. Although prior studies did not find a clear association between COX-2 and prognosis in penile cancer (De Paula et al., 2012), our data suggest that its overexpression is more pronounced in aggressive forms of the disease.

AIF-1, a protein involved in regulating inflammation, is also overexpressed in various cancers, including breast and liver, and is associated with worse outcomes (Liu et al., 2007, 2008; Zhang et al., 2018; De Leon-Oliva et al., 2023). It is known to activate pathways such as NF-κB and ß-catenin, which promote tumor growth (Jia et al., 2015), and our study observed elevated AIF-1 levels in more aggressive penile tumors, suggesting a potential link to prognosis.

Finally, NLRP3, a key component of the inflammasome, is involved in sensing cellular stress and triggering inflammatory responses through cytokines like IL-1ß and IL-18 (Rathinam and Chan, 2018). Although its role in cancer is complex, with some studies suggesting protective effects, NLPR3 is generally associated with cancer progression and poor prognosis (Swanson et al., 2019; Ortega et al., 2023b; Shadab et al., 2023). In our study, NLPR3 was more expressed in aggressive tumor subtypes, indicating its potential role in penile cancer progression, although further research is required to confirm its prognostic value.

These findings suggest that COX-2, AIF-1, and NLPR3 may serve as important inflammatory biomarkers in penile cancer, with potential links to tumor aggressiveness and patient outcomes.

Histopathological markers of autophagy and epigenetics in penile cancer

Autophagy is essential for cellular maintenance, regulating the removal of damaged components, and promoting responses to stress. It influences various cellular processes, including survival, proliferation, metabolism, and immune evasion, making it important in both normal cell function and cancer (Boya et al., 2013; Levine and Kroemer, 2019; Klionsky et al., 2021). While autophagy generally acts as a tumor-suppressive mechanism by eliminating damaged or toxic cellular components, it can also support tumor cells by maintaining metabolic fitness and aiding immune evasion (Mulcahy Levy and Thorburn, 2020; Yamamoto et al., 2020; Mukhopadhyay et al., 2021). Dysregulated autophagy is linked to several cancers, such as melanoma, breast cancer, and lung cancer (Saha, 2012; Artal-Martinez de Narvajas et al., 2013; Liu et al., 2013; Strohecker et al., 2013; Kim et al., 2018; Yamamoto et al., 2020).

In penile cancer, key proteins involved in autophagy, such as ULK-1 and ATG9A, have been shown to have elevated expression in more aggressive tumor stages. ULK-1, which initiates autophagy by forming a complex with ATG13 and RB1CC1/FIP200, is overexpressed in the aggressive P stage of penile carcinoma compared with less aggressive stages (Chan et al., 2007; Hara et al., 2008). This suggests that ULK-1 could be a biomarker and a therapeutic target for PSCC. Further research is needed to confirm its role in cancer progression.

While the expression of the ATG9A molecule has an important role as an autophagy-related protein responsible for lipid transport during autophagosome formation, it is also more highly expressed in aggressive stages of penile cancer (Bento et al., 2016). Its function in penile cancer is not yet fully understood, however, its elevated expression suggests that it may play a role in tumor aggressiveness, making it another potential biomarker for the disease.

Finally, HAT-1 is involved in regulating histone modification and cellular processes like DNA repair, it has been linked to various cancers and is associated with poor prognosis (Popova et al., 2021). Its acetyltransferase activity is regulated by AMPK, linking it to autophagy regulation (Ortega et al., 2023a). In penile cancer, HAT-1 also shows higher expression in aggressive stages, reinforcing its potential as a therapeutic target.

These findings suggest that autophagy-related molecules, including ULK-1, ATG9A, and HAT-1, may serve as important biomarkers and therapeutic targets in penile carcinoma. However, further studies are required to confirm their roles in cancer progression and treatment.

Correlation analysis and odds ratio estimation.

Our analysis of Figures 1-14 demonstrates a clear increase in marker expression across different histopathological groups, categorized by cell differentiation in PSCC. However, Figures 15-19 reveal diverse correlation patterns when examining the total cohort and subgroups based on disease subtype. This indicates that proteins do not show a consistent linear relationship across all tumor subtypes, suggesting distinct molecular mechanisms influencing tumor

progression and prognosis.

The variability in these protein correlations reflects differences in signaling pathways, cellular activities, and responses to treatments among PSCC subtypes. For instance, CDK4 and Cyclin D1 exhibit strong correlations in P and M tumor stages but not in W and V subtypes. In P tumors, CDK4 and Cyclin D1 are also associated with COX-2, promoting their coordinated role in cell cycle regulation. CDK4 correlated with ß-catenin in P and W tumors but interacted with NLRP3 in V tumors, while in P tumors, it showed a negative correlation with AIF-1. Also, autophagy-related proteins, such as ATG9A and ULK-1, correlate with NLRP3 in P and M subtypes, and these correlations are more pronounced in P tumors.

In contrast, V tumors, associated with a better prognosis, show more coordinated protein regulation. Cyclin D1 correlates with IRS-4, Ki-67, COX-2, and HAT-1 in V tumors, while COX-2 is linked to IRS-4, RB-1, HAT-1, and AIF-1. In W tumors, Cyclin D1 loses its correlations, and COX-2 associates more strongly with ß-catenin and ERBB2. IRS-4 shows varying associations across subtypes, correlating with Ki-67, V, W, and M stages but not in P tumors, where it correlates with RB-1. These findings suggest that the molecular interactions within each PSCC subtype are unique and could provide valuable insights for personalized therapies and prognoses.

Although our study emphasizes significant correlations, we must consider limitations such as sample size and variability in coefficient estimates. While the preliminary findings suggest that molecular features may contribute to the differentiation of PSCC subtypes, larger studies are needed to validate these correlations and improve our understanding of the clinical implications. Further exploration of other variables and larger cohorts will be important to draw more definite, generalizable conclusions.

Conclusions

In the present study, we have evaluated and demonstrated the existence of the differential expression of several biomarkers involved in cell proliferation and cell cycle (IRS-4, Ki-67, RB1, CDK4, cyclin D1, ERBB2, β-catenin, and MAGE-A), inflammation (COX-2, NLRP3, and AIF-1), epigenetics (HAT-1), and autophagy (ULK-1 and ATG9A) in penile carcinoma according to the degree of differentiation (P, M, W, and V). Overall, our results show that these molecules are more highly expressed in P and M squamous carcinomas compared with the more differentiated W and V subtypes. Thus, individually, these proteins should be evaluated and confirmed in future studies as biomarkers of worse prognosis. However, our results have also shown that there are significant differences in the correlation of the expression patterns of these molecules. This fact could be indicative of a distinctive regulatory network according to the degree of differentiation, thus explaining the possible biological differences between each subtype. Likewise, we have also shown that the study of the expression of these molecules could have important clinical value in stratifying the different PSCC subtypes, although further studies are required to confirm these findings and to make solid and generalizable statements.

Author Contributions. All authors have read and agreed to the published version of the manuscript.

Funding. This study was funded by the Community of Madrid (MITI-CM-P2022-BMD/7321, ProACapital, and HALEKULANI, S. L. and MJR.

Conflicts of Interest. The authors declare no conflicts of interest.

References

Artal-Martinez de Narvajas A., Gomez T.S., Zhang J.-S., Mann A.O., Taoda Y., Gorman J.A., Herreros-Villanueva M., Gress T.M., Ellenrieder V., Bujanda L., Kim D.-H., Kozikowski A. P., Koenig A. and Billadeau D.D. (2013). Epigenetic regulation of autophagy by the methyltransferase G9a. Mol. Cell. Biol. 33, 3983-3993.

Arteaga C.L. and Engelman J.A. (2014). ERBB receptors: from oncogene discovery to basic science to mechanism-based cancer therapeutics. Cancer Cell 25, 282-303.

Arya M., Thrasivoulou C., Henrique R., Millar M., Hamblin R., Davda R., Aare K., Masters J.R., Thomson C., Muneer A., Patel H.R.H. and Ahmed A. (2015). Targets of Wnt/ß-catenin transcription in penile carcinoma. PLoS One 10, e0124395.

Baker S.J. and Reddy E.P. (2012). CDK4: A key player in the cell cycle, development, and cancer. Genes Cancer 3, 658-669.

Bakhtiar R. (2017). Translational application of biomarkers. In: Targeted biomarker quantitation by LC–MS. Weng N. and Jian W. (eds). John Wiley & Sons. pp 17-33.

Bento C. F., Renna M., Ghislat G., Puri C., Ashkenazi A., Vicinanza M., Menzies F.M. and Rubinsztein D.C. (2016). Mammalian autophagy: How does it work? Annu. Rev. Biochem. 85, 685-713.

Berdjis N., Meye A., Nippgen J., Dittert D., Hakenberg O., Baretton G.B. and Wirth M.P. (2005). Expression of Ki-67 in squamous cell carcinoma of the penis. BJU Int. 96, 146-148.

Berry J.L., Polski A., Cavenee W.K., Dryja T.P., Linn Murphree A. and Gallie B.L. (2019). The RB1 story: Characterization and cloning of the first tumor suppressor gene. Genes 10, 879.

Borque-Fernando Á., Gaya J.M., Esteban-Escaño L.M., Gómez-Rivas J., García-Baquero R., Agreda-Castañeda F., Gallioli A., Verri P., Ortiz-Vico F.J., Amir-Nicolau B.F., Osman-Garcia I., Gil-Martínez P., Arrabal-Martín M., Gómez-Ferrer Lozano Á., Campos-Juanatey F., Guerrero-Ramos F. and Rubio-Briones J. (2023). Epidemiology, diagnosis and management of penile cancer: Results from the Spanish National Registry of Penile Cancer. Cancers 15, 616.

Boya P., Reggiori F. and Codogno P. (2013). Emerging regulation and functions of autophagy. Nat. Cell Biol. 15, 713-720.

Brouwer O.R., Albersen M., Parnham A., Protzel C., Pettaway C.A., Ayres B., Antunes-Lopes T., Barreto L., Campi R., Crook J., Fernández-Pello S., Greco I., van der Heijden M.S., Johnstone P.A.S., Kailavasan M., Manzie K., Marcus J.D., Necchi A., Oliveira P., Osborne J., Pagliaro L.C., Garcia-Perdomo H.A., Rumble R.B., Sachdeva A., Sakalis V.I., Zapalo Ł., Martínez D.F.S., Spiess P.E. and Tagawa S.T. (2023). European Association of Urology-

American Society of Clinical Oncology Collaborative Guideline on Penile Cancer: 2023 Update. Eur. Urol. 83, 548-560.

Chan E.Y.W., Kir S. and Tooze S.A. (2007). siRNA screening of the kinome identifies ULK1 as a multidomain modulator of autophagy. J. Biol. Chem. 282, 25464-25474.

Chaux A., Torres J., Pfannl R., Barreto J., Rodriguez I., Velazquez E.F. and Cubilla A.L. (2009). Histologic grade in penile squamous cell carcinoma visual estimation *versus* digital measurement of proportions of grades, adverse prognosis with any proportion of grade 3 and correlation of a gleason-like system with nodal metastasis. Am. J. Surg. Pathol. 33, 1042-1048.

Chinnam M. and Goodrich D.W. (2011). RB1, development, and cancer. Curr. Top. Dev. Biol. 94, 129-169.

Claude-Taupin A., Jia J., Bhujabal Z., Garfa-Traoré M., Kumar S., da Silva G.P.D., Javed R., Gu Y., Allers L., Peters R., Wang F., da Costa L.J., Pallikkuth S., Lidke K.A., Mauthe M., Verlhac P., Uchiyama Y., Salemi M., Phinney B., Tooze S.A., Mari M.C., Johansen T., Reggiori F. and Deretic V. (2021). ATG9A protects the plasma membrane from programmed and incidental permeabilization. Nat. Cell Biol. 23, 846-858.

Cruciat C.M. and Niehrs C. (2013). Secreted and transmembrane wnt inhibitors and activators. Cold Spring Harb. Perspect. Biol. 5, a015081.

Cuylen S., Blaukopf C., Politi A.Z., Muller-Reichert T., Neumann B., Poser I., Ellenberg J., Hyman A.A. and Gerlich D.W. (2016). Ki-67 acts as a biological surfactant to disperse mitotic chromosomes. Nature 535, 308-312.

Czajkowski M., Wierzbicki P.M., Kotulak-Chrząszcz A., Małkiewicz B., Sosnowski R., Kmieć Z. and Matuszewski M. (2023). Pro-Inflammatory cytokine gene expression in penile cancer: Preliminary studies. Medicina 59, 1623.

da Silva J., da Costa C.C., de Farias Ramos I., Laus A.C., Sussuchi L., Reis R.M., Khayat A.S., Cavalli L.R. and Pereira S.R. (2022). Upregulated miRNAs on the TP53 and RB1 binding seedless regions in high-risk HPV-associated penile cancer. Front. Genet. 13, 875939.

De Donato M., Peters S.O., Hussain T., Rodulfo H., Thomas B.N., Babar M.E. and Imumorin I.G. (2017). Molecular evolution of type II MAGE genes from ancestral MAGED2 gene and their phylogenetic resolution of basal mammalian clades. Mamm. Genome 28, 443-454.

De Leon-Oliva D. Garcia-Montero C. Fraile-Martinez O., Boaru D.L., García-Puente L., Rios-Parra A., Garrido-Gil M.J., Casanova-Martín C., García-Honduvilla N., Bujan J., Guijarro L.G., Alvarez-Mon M. and Ortega M.A. (2023). AIF1: Function and connection with inflammatory diseases. Biology 12, 694.

De Paula A.A.P., Motta E.D., Alencar R.D.C., Saddi V.A., Da Silva R.C., Caixeta G.N., Almeida Netto J.C. and Carneiro M.A.D.S. (2012). The impact of cyclooxygenase-2 and vascular endothelial growth factor C immunoexpression on the prognosis of penile carcinoma. J. Urol. 187, 134-140.

Denk D. and Greten F.R. (2022). Inflammation: the incubator of the tumor microenvironment. Trends Cancer 8, 901-914.

Douglawi A. and Masterson T.A. (2017). Updates on the epidemiology and risk factors for penile cancer. Transl. Androl. Urol. 6, 785.

Doyle J.M., Gao J., Wang J., Yang M. and Potts P.R. (2010). MAGE-RING protein complexes comprise a family of E3 ubiquitin ligases. Mol. Cell 39, 963-974.

Duffy M.J. (2013). Tumor markers in clinical practice: a review focusing on common solid cancers. Med. Princ. Pract. 22, 4-11.

Engelsgjerd J.S. and LaGrange C.A. (2022). Penile cancer and penile intraepithelial neoplasia. StatPearls. Publishing. Treasue Island. (Updated September 2, 2024).

Feitelson M.A., Arzumanyan A., Kulathinal R.J., Blain S.W., Holcombe R.F., Mahajna J., Marino M., Martinez-Chantar M.L., Nawroth R., Sanchez-Garcia I., Sharma D., Saxena N.K., Singh N., Vlachostergios P.J., Guo S., Honoki K., Fujii H., Georgakilas A.G., Amedei A., Niccolai E., Amin A., Ashraf S.S., Boosani C.S., Guha G., Ciriolo M.R., Aquilano K., Chen S., Mohammed S.I., Azmi A.S., Bhakta D., Halicka D., Keith W.N. and Nowsheen S. (2015). Sustained proliferation in cancer: mechanisms and novel therapeutic targets. Semin. Cancer Biol, 35, 25-54.

Fenner F., Goody D., Protzel C., Erbersdobler A., Richter C., Hartz J.M., Naumann C.M., Kalthoff H., Herchenröder O., Hakenberg O.W. and Pützer B.M. (2018). E2F1 Signalling is predictive of chemoresistance and lymphogenic metastasis in penile cancer: A pilot functional study reveals new prognostic biomarkers. Eur. Urol. Focus 4, 599-607.

Fraile-Martinez O. García-Montero C., Pekarek L., Saz J.V., Alvarez-Mon M.Á., Barrena-Blázquez S., García-Honduvilla N., Buján J., Asúnsolo Á., Coca S., Alvarez-Mon M., Guijarro L.G., Saez M.A. and Ortega M.A. (2023). Decreased survival in patients with pancreatic cancer may be associated with an increase in histopathological expression of inflammasome marker NLRP3. Histol. Histopathol. 39, 35-40.

Gerdes J., Schwab U., Lemke H. and Stein H. (1983). Production of a mouse monoclonal antibody reactive with a human nuclear antigen associated with cell proliferation. Int. J. Cancer 31, 13-20.

Goel S., Bergholz J.S. and Zhao J.J. (2022). Targeting cyclin-dependent kinases 4 and 6 in cancer. Nat. Rev. Cancer 22, 356.

Greten F.R. and Grivennikov S.I. (2019). Inflammation and cancer: Triggers, mechanisms, and consequences. Immunity 51, 27-41.

Guijarro L.G., Justo Bermejo F.J., Boaru D.L., De Castro-Martinez P., De Leon-Oliva D., Fraile-Martínez O., Garcia-Montero C., Alvarez-Mon M., Toledo-Lobo M. del V. and Ortega M.A. (2023). Is Insulin Receptor Substrate4 (IRS4) a platform involved in the activation of several oncogenes? Cancers 15, 4651.

Guimarães G.C., de Oliveira Leal M.L., Sousa Madeira Campos R., de Cássio Zequi S., da Fonseca F.P., da Cunha I.W., Soares F.A. and Lopes A. (2007). Do proliferating cell nuclear antigen and MIB-1/Ki-67 have prognostic value in penile squamous cell carcinoma? Urology 70, 137-142.

Hagiwara Y., Sieverling L., Hanif F., Anton J., Dickinson E.R., Bui T.T.T., Andreeva A., Barran P.E., Cota E. and Nikolova P.V. (2016). Consequences of point mutations in melanoma-associated antigen 4 (MAGE-A4) protein: Insights from structural and biophysical studies. Sci. Rep. 6, 25182.

Hakenberg O.W., Compérat E. M., Minhas S., Necchi A., Protzel C. and Watkin N. (2015). EAU guidelines on penile cancer: 2014 Update. Eur. Urol. 67, 142-150.

Hakenberg O.W., Dräger D.L., Erbersdobler A., Naumann C.M., Jünemann K.P. and Protzel C. (2018). The diagnosis and treatment of penile cancer. Dtsch. Arztebl. Int. 115, 646-652.

Hamilton E. and Infante J.R. (2016). Targeting CDK4/6 in patients with cancer. Cancer Treat. Rev. 45, 129-138.

Hanahan D. (2022). Hallmarks of cancer: New dimensions. Cancer Discov. 12, 31-46.

Hanahan D. and Weinberg R.A. (2011). Hallmarks of cancer: The next

generation. Cell 144, 646-674.

Hao Y.H., Doyle J.M., Ramanathan S., Gomez T.S., Jia D., Xu M., Chen Z.J., Billadeau D.D., Rosen M.K. and Potts P.R. (2013). Regulation of WASH-dependent actin polymerization and protein trafficking by ubiquitination. Cell 152, 1051-1064.

Hao P., Huang Y., Peng J., Yu J., Guo X., Bao F., Dian Z., An S. and Xu T.-R. (2021). IRS4 promotes the progression of non-small cell lung cancer and confers resistance to EGFR-TKI through the activation of PI3K/Akt and Ras-MAPK pathways. Exp. Cell Res. 403, 112615.

Hara T., Takamura A., Kishi C., Iemura S.I., Natsume T., Guan J.L. and Mizushima N. (2008). FIP200, a ULK-interacting protein, is required for autophagosome formation in mammalian cells. J. Cell Biol. 181, 497-510.

Hashemi Goradel N., Najafi M., Salehi E., Farhood B. and Mortezaee K. (2019). Cyclooxygenase-2 in cancer: A review. J. Cell. Physiol. 234, 5683-5699.

Hooper M.L. (1994). The role of the p53 and Rb-1 genes in cancer, development and apoptosis. J. Cell Sci. (Suppl. 18), 13-17.

Huang K.-B., Liu R.-Y., Peng Q.-H., Li Z.-S., Jiang L.-J., Guo S.-J ., Zhou Q.-H., Liu T.-Y., Deng C.-Z.,. Yao K., Qin Z.-K., Liu Z.-W., Li Y.-H., Han H. and Zhou F.-J. (2019). EGFR mono-antibody salvage therapy for locally advanced and distant metastatic penile cancer: Clinical outcomes and genetic analysis. Urol. Oncol. 37, 71-77.

Hudolin T., Juretic A., Pasini J., Tomas D., Spagnoli G.C., Heberer M., Dimanovski J. and Kruslin B. (2006). Immunohistochemical expression of tumor antigens MAGE-A1, MAGE-A3/4, and NY-ESO-1 in squamous cell carcinoma of the penis. Urology 68, 205-207.

Indovina P., Pentimalli F., Casini N., Vocca I. and Giordano A. (2015). RB1 dual role in proliferation and apoptosis: cell fate control and implications for cancer therapy. Oncotarget 6, 17873-17890.

Ioachim E. (2008). Expression patterns of cyclins D1, E and cyclin-dependent kinase inhibitors p21waf1/cip1, p27kip1 in colorectal carcinoma: Correlation with other cell cycle regulators (pRb, p53 and Ki-67 and PCNA) and clinicopathological features. Int. J. Clin. Pract. 62, 1736-1743.

Iorga L., Marcu R.D., Diaconu C.C., Stanescu A.M.A., Stoian A.P., Mischianu D.L. D., Surcel M., Bungau S., Constantin T., Boda D., Fekete L. and Bratu O.G. (2020). Penile carcinoma and HPV infection (Review). Exp. Ther. Med. 20, 91-96.

Janicic A., Petrovic M., Zekovic M., Vasilic N., Coric V., Milojevic B., Zivkovic M. and Bumbasirevic U. (2023). Prognostic significance of systemic inflammation markers in testicular and penile cancer: A narrative review of current literature. Life 13, 600.

Jia S., Du Z., Jiang H., Huang X., Chen Z. and Chen N. (2015). Daintain/AIF-1 accelerates the activation of insulin-like growth factor-1 receptor signaling pathway in HepG2 cells. Oncol. Rep. 34, 511-517.

Kellas-Ślęczka S., Białas B., Fijałkowski M., Wojcieszek P., Szlag M., Cholewka A., Wesołowski M., Ślęczka M., Krzysztofiak T., Larysz D., Kołosza Z., Trzaska K. and Pruefer A. (2019). Nineteen-year single-center experience in 76 patients with penile cancer treated with high-dose-rate brachytherapy. Brachytherapy 18, 493-502.

Kim T.W., Lee S.Y., Kim M., Cheon C. and Ko S.G. (2018). Kaempferol induces autophagic cell death via IRE1-JNK-CHOP pathway and inhibition of G9a in gastric cancer cells. Cell Death Dis. 9, 875.

Klionsky D.J., Petroni G., Amaravadi R.K., Baehrecke E.H., Ballabio A., Boya P., Bravo-San Pedro J.M., Cadwell K., Cecconi F., Choi A.M.K., Choi M.E., Chu C.T., Codogno P., Colombo M.I., Cuervo A.M., Deretic V., Dikic I., Elazar Z., Eskelinen E., Fimia G.M., Gewirtz D.A., Green D.R., Hansen M., Jäättelä M., Johansen T., Juhász G., Karantza V., Kraft C., Kroemer G., Ktistakis N.T., Kumar S., Lopez-Otin C., Macleod K.F., Madeo F., Martinez J., Meléndez A., Mizushima N., Münz C., Penninger J.M., Perera R.M., Piacentini M., Reggiori F., Rubinsztein D.C., Ryan K.M., Sadoshima J., Santambrogio L., Scorrano L., Simon H.-U., Simon A.K., Simonsen A., Stolz A., Tavernarakis N., Tooze S.A., Yoshimori T., Yuan J., Yue Z., Zhong Q., Lorenzo Galluzzi and Pietrocola F. (2021). Autophagy in major human diseases. EMBO J. 40, e108863.

Kranz, J., Bartoletti, R., Bruyère, F., Cai, T., Geerlings, S., Köves, B., Schubert, S., Pilatz, A., Veeratterapillay, R., Wagenlehner, F. M. E., Bausch, K., Devlies, W., Horváth, J., Leitner, L., Mantica, G., Mezei, T., Smith, E. J., & Bonkat, G. (2024). European Association of Urology Guidelines on Urological Infections: Summary of the 2024 Guidelines. Eur Urol. 86, 2741.

Kuasne H., Do Canto L.M., Aagaard M.M., Muñoz J.J.M., De Jamblinne C., Marchi F. A., Scapulatempo-Neto C., Faria E.F., Lopes A., Carréno S. and Rogatto S.R. (2021). Penile cancer-derived cells molecularly characterized as models to guide targeted therapies. Cells 10, 814.

Leiter A., Veluswamy R.R. and Wisnivesky J. P. (2023). The global burden of lung cancer: current status and future trends. Nat. Rev. Clin. Oncol. 20, 624-639.

Levine B. and Kroemer G. (2019). Biological functions of autophagy genes: A disease perspective. Cell 176, 11-42.

Li F., Xu Y., Wang H., Chen B., Wang Z., Zhao Y., Zhu S. and Chen G. (2015). Diagnosis and treatment of penile verrucous carcinoma. Oncol. Lett. 9, 1687-1690.

Liu G., Ma H., Jiang L. and Zhao Y. (2007). Allograft inflammatory factor-1 and its immune regulation. Autoimmunity 40, 95-102.

Liu S., Tan W.Y., Chen Q.R., Chen X.P., Fu K., Zhao Y.Y. and Chen Z.W. (2008). Daintain/AIF-1 promotes breast cancer proliferation via activation of the NF-kappaB/cyclin D1 pathway and facilitates tumor growth. Cancer Sci. 99, 952-957.

Liu H., He Z., Von Rütte T., Yousefi S., Hunger R. E. and Simon H.U. (2013). Down-regulation of autophagy-related protein 5 (ATG5) contributes to the pathogenesis of early-stage cutaneous melanoma. Sci. Transl. Med. 5, 202ra123.

Liu S.G., Wu X.X., Hua T., Xin X.Y., Feng D.L., Chi S.Q., Wang X.X. and Wang H.B. (2019). NLRP3 inflammasome activation by estrogen promotes the progression of human endometrial cancer. Onco. Targets Ther. 12, 6927-6936.

Liu J., Xiao Q., Xiao J., Niu C., Li Y., Zhang X., Zhou Z., Shu G. and Yin G. (2022). Wnt/β-catenin signalling: function, biological mechanisms, and therapeutic opportunities. Signal Transduct. Target Ther. 7, 3.

Liu N., Wu T., Ma Y., Cheng H., Li W. and Chen M. (2023). Identification and validation of RB1 as an immune-related prognostic signature based on tumor mutation burdens in bladder cancer. Anticancer Drugs 34, 269-280.

Macedo J., Silva E., Nogueira L., Coelho R., da Silva J., dos Santos A., Teixeira-Júnior A.A., Belfort M., Silva G., Khayat A., de Oliveira E., dos Santos A.P., Cavalli L.R. and Pereira S.R. (2020). Genomic profiling reveals the pivotal role of hrHPV driving copy number and gene expression alterations, including mRNA downregulation of TP53 and RB1 in penile cancer. Mol. Carcinog. 59, 604-617.

Marchi F.A., Martins D.C., Barros-Filho M.C., Kuasne H., Busso Lopes A.F., Brentani H., Trindade Filho J.C.S., Guimarães G.C., Faria E.F., Scapulatempo-Neto C., Lopes A. and Rogatto S.R. (2017).

Multidimensional integrative analysis uncovers driver candidates and biomarkers in penile carcinoma. Sci. Rep. 7, 6707.

Matthews H.K., Bertoli C. and de Bruin R.A.M. (2021). Cell cycle control in cancer. Nat. Rev. Mol. Cell Biol. 23, 74-88.

McDaniel A.S., Hovelson D.H., Cani A.K., Liu C.J., Zhai Y., Zhang Y., Weizer A.Z., Mehra R., Feng F.Y., Alva A.S., Morgan T.M., Montgomery J.S., Siddiqui J., Sadis S., Bandla S., Williams P.D., Cho K.R., Rhodes D.R. and Tomlins S.A. (2015). Genomic profiling of penile squamous cell carcinoma reveals new opportunities for targeted therapy. Cancer Res. 75, 5219-5227.

Mehdi H.K., Raju K. and Sheela S.R. (2023). Association of P16, Ki-67, and CD44 expression in high-grade squamous intraepithelial neoplasia and squamous cell carcinoma of the cervix. J. Cancer Res. Ther. 19 (Supplement), S260-S267.

Miller I., Min M., Yang C., Tian C., Gookin S., Carter D. and Spencer S.L. (2018). Ki67 is a graded rather than a binary marker of proliferation *versus* quiescence. Cell Rep. 24, 1105.

Miller D.R., Ingersoll M.A. and Lin M.F. (2019). ErbB-2 signaling in advanced prostate cancer progression and potential therapy. Endocr. Relat. Cancer 26, R195-R209.

Miranda E.I. (2010). MAGE, biological functions and potential clinical applications. Leuk. Res. 34, 1121-1122.

Mirzaa G.M., Parry D.A., Fry A.E., Giamanco K.A., Schwartzentruber J., Vanstone M., Logan C.V., Roberts N., Johnson C.A., Singh S., Kholmanskikh S.S., Adams C., Hodge R.D., Hevner R.F., Bonthron D.T., Braun K.P.J., Faivre L., Rivière J.B., St-Onge J., Gripp K.W., Mancini G.M., Pang K., Sweeney E., van Esch H., Verbeek N., Wieczorek D., Steinraths M., Majewski J., FORGE Canada Consortium, Boycot K.M., Pilz D.T., Ross M.E., Dobyns W.B., Sheridan E.G. and Scherer S. (2014). De novo CCND2 mutations leading to stabilization of cyclin D2 cause megalencephaly-polymicrogyria-polydactyly-hydrocephalus syndrome. Nat. Genet. 46, 510-515.

Montalto F.I. and De Amicis F. (2020). Cyclin D1 in cancer: A molecular connection for cell cycle control, adhesion and invasion in tumor and stroma. Cells 9, 2648.

Montella M., Sabetta R., Ronchi A., De Sio M., Arcaniolo D., De Vita F., Tirino G., Caputo A., D'Antonio A., Fiorentino F., Facchini G., Lauro G. Di Perdonà S., Ventriglia J., Aquino G., Feroce F., Borges Dos Reis R., Neder L., Brunelli M., Franco R. and Marino F.Z. (2022). Immunotherapy in penile squamous cell carcinoma: Present or future? Multi-target analysis of programmed cell death ligand 1 expression and microsatellite instability. Front. Med. 9, 874213.

Morrison B.F. (2014). Risk factors and prevalence of penile cancer. West Indian Med. J. 63, 559-560.

Mukhopadhyay S., Biancur D.E., Parker S.J., Yamamoto K., Banh R.S., Paulo J.A., Mancias J.D. and Kimmelman A.C. (2021). Autophagy is required for proper cysteine homeostasis in pancreatic cancer through regulation of SLC7A11. Proc. Natl. Acad. Sci. USA 118, e2021475118.

Mulcahy Levy J.M. and Thorburn A. (2020). Autophagy in cancer: Moving from understanding mechanism to improving therapy responses in patients. Cell Death Differ. 27, 843-857.

Newman J.A., Cooper C.D.O., Roos A.K., Aitkenhead H., Oppermann U.C.T., Cho H. J., Osman R. and Gileadi O. (2016). Structures of two melanoma-associated antigens suggest allosteric regulation of effector binding. PLoS One 11, e0148762.

Niehrs C. and Acebron S.P. (2012). Mitotic and mitogenic Wnt signalling. EMBO J. 31, 2705-2713.

Olesen T.B., Sand F.L., Rasmussen C.L., Albieri V., Toft B.G., Norrild B., Munk C. and Kjær S.K. (2019). Prevalence of human papillomavirus DNA and p16INK4a in penile cancer and penile intraepithelial neoplasia: A systematic review and meta-analysis. Lancet Oncol. 20, 145-158.

Ortega M.A., Fraile-Martínez O., Pekarek L., Alvarez-Mon M.A., Asúnsolo Á., Sanchez-Trujillo L., Coca S., Buján J., Álvarez-Mon M., García-Honduvilla N. and Sainz F. (2021). Defective expression of the peroxisome regulators PPARα receptors and lysogenesis with increased cellular senescence in the venous wall of chronic venous disorder. Histol. Histopathol. 36, 547-558.

Ortega M.A., Pekarek L., Fraile-Martinez O., Garcia-Montero C., Saez M. A., Asúnsolo A., Alvarez-Mon M.A., Monserrat J., Ruiz-Llorente L., García-Honduvilla N., Albillos A., Buján J., Alvarez-Mon M. and Guijarro L.G. (2022a). Implication of ERBB2 as a predictive tool for survival in patients with pancreatic cancer in histological studies. Curr. Oncol. 29, 2442-2453.

Ortega M.A., Pekarek L., Garcia-Montero C., Fraile-Martinez O., Saez M.A., Asúnsolo A., Alvarez-Mon M.A., Monserrat J., Coca S., Toledo-Lobo M.V., García-Honduvilla N., Albillos A., Buján J., Alvarez-Mon M. and Guijarro L.G. (2022b). Prognostic role of IRS-4 in the survival of patients with pancreatic cancer. Histol. Histopathol. 37, 449-459.

Ortega M.A., De Leon-Oliva D., García-Montero C., Fraile-Martinez O., Boaru D.L., de Castro A. V., Saez M.A., Lopez-Gonzalez L., Bujan J., Alvarez-Mon M.A., García-Honduvilla N., Diaz-Pedrero R. and Alvarez-Mon M. (2023a). Reframing the link between metabolism and NLRP3 inflammasome: Therapeutic opportunities. Front. Immunol. 14, 1232629.

Ortega M.A., De Leon-Oliva D., Garcia-Montero C., Fraile-Martinez O., Boaru D.L., del Val Toledo Lobo M., García-Tuñón I., Royuela M., García-Honduvilla N., Bujan J., Guijarro L.G., Alvarez-Mon M. and Alvarez-Mon M.Á. (2023b). Understanding HAT1: A comprehensive review of noncanonical roles and connection with disease. Genes 14, 915.

Ortiz J.F., Ruxmohan S., Khurana M., Hidalgo J., Alzamora I.M. and Patel A. (2021). Megalencephaly polymicrogyria polydactyly hydrocephalus (MPPH): A case report and review of literature. Cureus 13, e16132.

Padayachee J., Daniels A., Balgobind A., Ariatti M. and Singh M. (2020). *HER-2/neu* and *MYC* gene silencing in breast cancer: therapeutic potential and advancement in nonviral nanocarrier systems. Nanomedicine 15, 1437-1452.

Paternot S., Bockstaele L., Bisteau X., Kooken H., Coulonval K. and Roger P.P. (2010). Rb inactivation in cell cycle and cancer: the puzzle of highly regulated activating phosphorylation of CDK4 *versus* constitutively active CDK-activating kinase. Cell Cycle 9, 689-699.

Pekarek L., Ortega M.A., Fraile-Martinez O., García-Montero C., Casanova C., Saez M. A., García-Honduvilla N., Alvarez-Mon M., Buján J., Diez-Nicolas V., Burgos J.F., and Gomez Dos Santos V. (2022). Clinical and novel biomarkers in penile carcinoma: A prospective review. J. Pers. Med. 12, 1364.

Perugorria M.J., Olaizola P., Labiano I., Esparza-Baquer A., Marzioni M., Marin J.J.G., Bujanda L. and Banales J.M. (2019). Wnt-β-catenin signalling in liver development, health and disease. Nat. Rev. Gastroenterol. Hepatol. 16, 121-136.

Popova L.V., Nagarajan P., Lovejoy C.M., Sunkel B.D., Gardner M.L., Wang M., Freitas M.A., Stanton B.Z. and Parthun M.R. (2021).

Epigenetic regulation of nuclear lamina-associated heterochromatin by HAT1 and the acetylation of newly synthesized histones. Nucleic Acids Res. 49, 12136-12151.

Poziello A., Nebbioso A., Stunnenberg H.G., Martens J.H.A., Carafa V. and Altucci L. (2021). Recent insights into Histone Acetyltransferase-1: biological function and involvement in pathogenesis. Epigenetics 16, 838-850.

Protzel C. and Hakenberg O.W. (2020). Penile cancer: Diagnosis and treatment. Urologe A. 59, 209-218. (Article in German).

Protzel C. and Spiess P.E. (2013). Molecular research in penile cancer—Lessons learned from the past and bright horizons of the future? Int. J. Mol. Sci. 14, 19494.

Purnama A., Lukman K., Rudiman R., Prasetyo D., Fuadah Y., Nugraha P. and Candrawinata V.S. (2023). The prognostic value of COX-2 in predicting metastasis of patients with colorectal cancer: A systematic review and meta analysis. Heliyon 9, e21051.

Raghav K.P.S. and Moasser M.M. (2023). Molecular pathways and mechanisms of HER2 in cancer therapy. Clin. Cancer Res. 29, 2351-2361.

Rathinam V.A.K. and Chan F.K.M. (2018). Inflammasome, inflammation and tissue homeostasis. Trends Mol. Med. 24, 304.

Ren W. and Gu G. (2017). Prognostic implications of RB1 tumour suppressor gene alterations in the clinical outcome of human osteosarcoma: a meta-analysis. Eur. J. Cancer Care (Engl), 26.

Reuschenbach M., Seiz M., Von Knebel Doeberitz C., Vinokurova S., Duwe A., Ridder R., Sartor H., Kommoss F., Schmidt D. and Doeberitz M.V.K. (2012). Evaluation of cervical cone biopsies for coexpression of p16INK4a and Ki-67 in epithelial cells. Int. J. Cancer 130, 388-394.

Roskoski R. (2019). Small molecule inhibitors targeting the EGFR/ErbB family of protein-tyrosine kinases in human cancers. Pharmacol. Res. 139, 395-411.

Saha T. (2012). LAMP2A overexpression in breast tumors promotes cancer cell survival via chaperone-mediated autophagy. Autophagy 8, 1643.

Sanchez D.F., Soares F., Alvarado-Cabrero I., Cañete S., Fernández-Nestosa M.J., Rodríguez I.M., Barreto J. and Cubilla A.L. (2015). Pathological factors, behavior, and histological prognostic risk groups in subtypes of penile squamous cell carcinomas (SCC). Semin. Diagn. Pathol. 32, 222-231.

Sekhoacha M., Riet K., Motloung P., Gumenku L., Adegoke A. and Mashele S. (2022). Prostate cancer review: Genetics, diagnosis, treatment options, and alternative approaches. Molecules 27, 5730.

Shadab A., Mahjoor M., Abbasi-Kolli M., Afkhami H., Moeinian P. and Safdarian A.R. (2023). Divergent functions of NLRP3 inflammasomes in cancer: a review. Cell Commun. Signal. 21, 1-15.

Shaw L.M. (2011). The insulin receptor substrate (IRS) proteins: at the intersection of metabolism and cancer. Cell Cycle 10, 1750-1756.

Shen J., Dong J., Shao F., Zhao J., Gong L., Wang H., Chen W., Zhang Y. and Cai Y. (2022). Graphene oxide induces autophagy and apoptosis via the ROS-dependent AMPK/mTOR/ULK-1 pathway in colorectal cancer cells. Nanomedicine 17, 591-605.

Shin A.E., Giancotti F.G. and Rustgi A.K. (2023). Metastatic colorectal cancer: mechanisms and emerging therapeutics. Trends Pharmacol. Sci. 44, 222-236.

Singh N., Baby D., Rajguru J., Patil P., Thakkannavar S. and Pujari V. (2019). Inflammation and cancer. Ann. Afr. Med. 18, 121.

Sobecki M., Mrouj K., Camasses A., Parisis N., Nicolas E., Llères D., Gerbe F., Prieto S., Krasinska L., David A., Eguren M., Birling M.C., Urbach S., Hem S., Déjardin J., Malumbres M., Jay P., Dulic V., Lafontaine D.L.J., Feil R. and Fisher D. (2016). The cell proliferation antigen Ki-67 organises heterochromatin. Elife 5, e13722.

Stankiewicz E., Ng M., Cuzick J., Mesher D., Watkin N., Lam W., Corbishley C. and Berney D.M. (2012). The prognostic value of Ki-67 expression in penile squamous cell carcinoma. J. Clin. Pathol. 65, 534-537.

Strohecker A.M., Guo J.Y., Karsli-Uzunbas G., Price S.M., Chen G.J., Mathew R., McMahon M. and White E. (2013). Autophagy sustains mitochondrial glutamine metabolism and growth of BrafV600E-driven lung tumors. Cancer Discov. 3, 1272-1285.

Sun X., Bizhanova A., Matheson T.D., Yu J., Zhu L.J. and Kaufman P.D. (2017). Ki-67 contributes to normal cell cycle progression and inactive X heterochromatin in p21 checkpoint-proficient human cells. Mol. Cell Biol. 37, e00569.

Sun X. and Kaufman P.D. (2018). Ki-67: More than a proliferation marker. Chromosoma 127, 175-186.

Suryadinata R., Sadowski M. and Sarcevic B. (2010). Control of cell cycle progression by phosphorylation of cyclin-dependent kinase (CDK) substrates. Biosci. Rep. 30, 243-255.

Swanson K.V., Deng M. and Ting J.P.Y. (2019). The NLRP3 inflammasome: Molecular activation and regulation to therapeutics. Nat. Rev. Immunol. 19, 477-489.

Tan X., Wang Y., Wu Z., Zhou Q., Tang Y., Liu Z., Yuan G., Luo S., Zou Y., Guo S., Han N. and Yao K. (2023). The role of Her-2 in penile squamous cell carcinoma progression and cisplatin chemoresistance and potential for antibody-drug conjugate-based therapy. Eur. J. Cancer 194, 113360.

Teixeira Júnior A.A.L., da Costa Melo S.P., Pinho J.D., Sobrinho T.B.M., Rocha T.M.S., Duarte D.R.D., de Oliveira Barbosa L., Duarte W.E., de Castro Belfort M.R., Duarte K.G., da Silva Neto A.L., de Ribamar Rodrigues Calixto J., Paiva Paiva L.C., do Nascimento F.S.M.S., Alencar Junior A.M., Khayat A.S., da Graça Carvalhal Frazão Corrêa R., Lages J.S., dos Reis R.B., Araújo W.S, Jr. and Silva G.E.B. (2022). A comprehensive analysis of penile cancer in the region with the highest worldwide incidence reveals new insights into the disease. BMC Cancer 22, 1063.

Thomas A., Necchi A., Muneer A., Tobias-Machado M., Tran A.T.H., Van Rompuy A. S., Spiess P.E. and Albersen M. (2021a). Penile cancer. Nat. Rev. Dis. Primers 7, 11.

Thomas A., Reetz S., Stenzel P., Tagscherer K., Roth W., Schindeldecker M., Michaelis M., Rothweiler F., Cinatl J., Cinatl J., Dotzauer R., Vakhrusheva O., Albersen M., Macher-Goeppinger S., Haferkamp A., Juengel E., Neisius A. and Tsaur I. (2021b). Assessment of PI3K/mTOR/AKT pathway elements to serve as biomarkers and therapeutic targets in penile cancer. Cancers 13, 2323.

Urruticoechea A., Smith I.E. and Dowsett M. (2005). Proliferation marker Ki-67 in early breast cancer. J. Clin. Oncol. 23, 7212-7220.

Velazquez E.F., Ayala G., Liu H., Chaux A., Zanotti M., Torres J., Cho S.I., Barreto J.E., Soares F. and Cubilla A.L. (2008). Histologic grade and perineural invasion are more important than tumor thickness as predictor of nodal metastasis in penile squamous cell carcinoma invading 5 to 10 mm. Am. J. Surg. Pathol. 32, 974-979.

Verhoeven R.H.A., Janssen-Heijnen M.L.G., Saum K.U., Zanetti R., Caldarella A., Holleczek B., Brewster D.H., Hakulinen T., Horenblas S., Brenner H. and Gondos A. (2013). Population-based survival of penile cancer patients in Europe and the United States of America: no improvement since 1990. Eur. J. Cancer 49, 1414-1421.

Visconti R., Della Monica R. and Grieco D. (2016). Cell cycle checkpoint in cancer: A therapeutically targetable double-edged sword. J. Exp. Clin. Cancer Res. 35, 153.

Wei L., Huang K., Han H. and Liu R.Y. (2023). Human papillomavirus infection in penile cancer: Multidimensional mechanisms and vaccine strategies. Int. J. Mol. Sci. 24, 16808.

Weon J.L. and Potts P.R. (2015). The MAGE protein family and cancer. Curr. Opin. Cell Biol. 37, 1-8.

White M.F. and Kahn C.R. (2021). Insulin action at a molecular level - 100 years of progress. Mol. Metab. 52, 101304.

Xie B., Tan G., Ren J., Lu W., Pervaz S., Ren X., Otoo A.A., Tang J., Li F., Wang Y. and Wang M. (2022). RB1 is an immune-related prognostic biomarker for ovarian Cancer. Front. Oncol. 12, 830908.

Yamamoto K., Venida A., Yano J., Biancur D.E., Kakiuchi M., Gupta S., Sohn A.S.W., Mukhopadhyay S., Lin E.Y., Parker S. J., Banh R.S., Paulo J.A., Wen K.W., Debnath J., Kim G.E., Mancias J.D., Fearon D.T., Perera R.M. and Kimmelman A.C. (2020). Autophagy promotes immune evasion of pancreatic cancer by degrading MHC-I. Nature 581, 100-105.

Yarden Y. and Pines G. (2012). The ERBB network: at last, cancer therapy meets systems biology. Nat. Rev. Cancer 12, 553-563.

Yu F., Yu C., Li F., Zuo Y., Wang Y., Yao L., Wu C., Wang C. and Ye L. (2021). Wnt/β-catenin signaling in cancers and targeted therapies. Signal Transduct. Target. Ther. 6, 307.

Yun Y.R., Won J.E., Jeon E., Lee S., Kang W., Jo H., Jang J.H., Shin U.S. and Kim H.W. (2010). Fibroblast growth factors: Biology, function, and application for tissue Regeneration. J. Tissue Eng, 2010, 218142.

Zhan X., Chen L., Jiang M. and Fu B. (2022). Get insight into the cause of death distribution and epidemiology of penile squamous cell carcinoma: A population-based study. Cancer Med. 11, 2308-2319.

Zhang Q., Sun S., Zhu C., Xie F., Cai Q., Sun H., Chen G., Liang X., Xie H., Shi J., Liao Y. and Zhou J. (2018). Expression of Allograft Inflammatory Factor-1 (AIF-1) in hepatocellular carcinoma. Med. Sci. Monit. 24, 6218-6228.

Zhang Y. and Wang X. (2020). Targeting the Wnt/β-catenin signaling pathway in cancer. J. Hematol. Oncol. 13, 165.

Zhang Q., Wu L., Liu S., Chen Q., Zeng L. and Chen X. (2021). Moderating hypoxia and promoting immunogenic photodynamic therapy by HER-2 nanobody conjugate nanoparticles for ovarian cancer treatment. Nanotechnology, 32.

Zhao Y.Y., Yan D.J. and Chen Z.W. (2013). Role of AIF-1 in the regulation of inflammatory activation and diverse disease processes. Cell. Immunol. 284, 75-83.

Zhu Y., Zhu X., Wei X., Tang C. and Zhang W. (2021). HER2-targeted therapies in gastric cancer. Biochim. Biophys. Acta Rev. Cancer 1876, 188549.

Accepted November 7, 2024

Penile carcinoma cancer

Supplementary material:

Justification of the result of the baseline principal component analysis (PCA) according to the standard deviations, the proportion contributed by each component to the variance of the data and the cumulative proportion.

```
Importance of components:
                          PC1     PC2     PC3     PC4     PC5     PC6     PC7     PC8
Standard deviation     3.3545 0.99167 0.66945 0.54398 0.48910 0.42782 0.40361 0.34351
Proportion of Variance 0.8038 0.07024 0.03201 0.02114 0.01709 0.01307 0.01164 0.00843
Cumulative Proportion  0.8038 0.87400 0.90601 0.92715 0.94424 0.95731 0.96895 0.97738
                          PC9    PC10    PC11    PC12    PC13    PC14
Standard deviation     0.30783 0.25138 0.2454 0.20639 0.1714 0.1631
Proportion of Variance 0.00677 0.00451 0.0043 0.00304 0.0021 0.0019
Cumulative Proportion  0.98414 0.98866 0.9930 0.99600 0.9981 1.0000
```

MS1. PCA results with standard deviations and their variance ratios from the first principal component to the last.

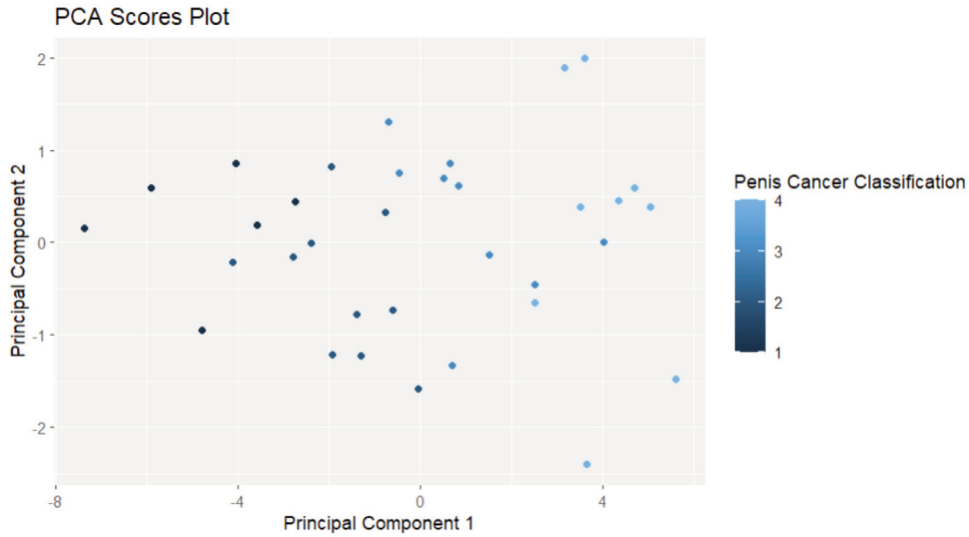

MS2. Screen plot to visualize the variance explained by the first two principal components

```
> # Obtener los loadings para PC1 y PC2
> loadings <- pca_result$rotation[, 1:2]
> # Mostrar los loadings
> print(loadings)
                      PC1         PC2
RB1            0.2609266 -0.27051100
COX2           0.2783096 -0.15452646
CDK4           0.2783832 -0.29373914
CYCLIN D1      0.2591034 -0.36249274
ERB2           0.2687899 -0.31318140
B-CATENIN 1    0.2731155 -0.21747431
MAGE           0.2765415 -0.11241142
HAT-1          0.2968903  0.16861469
AIF-1          0.2713804  0.38230250
NLRP3          0.2880007  0.26727111
ULK-1          0.2845742  0.35957493
ATG9A          0.2749863  0.37895706
Grupo_numerado 0.2918535  0.09124234
```

MS3. Loadings for PC1 and PC2. Contribution of each original protein or variable to the corresponding principal component in the PCA. IRS-4 and Ki-67 have been excluded in the dimensionality reduction process, indicating that their contribution to the total variability is minimal compared to the proteins included in the analysis.